

Desulfurization of Diesel Using Ionic Liquids: Process Design and Optimization Using COSMO-Based Models and Aspen Plus

Haifa Ben Salah, Paul Nancarrow,* and Amani Al Othman

Cite This: *ACS Omega* 2023, 8, 30001–30023

Read Online

ACCESS |



Metrics & More

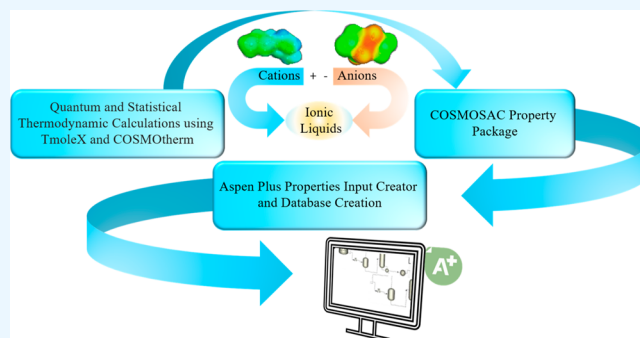


Article Recommendations



Supporting Information

ABSTRACT: Sulfur dioxide emissions from fossil fuel combustion have been known to cause detrimental health and environmental effects. The currently used hydrodesulfurization (HDS) method employed by refineries has several drawbacks, such as excessive hydrogen consumption, high energy demand, and inability to remove complex organosulfur compounds, which have limited its ability to produce ultralow sulfur diesel (ULSD) at reasonable operating and capital costs. Ionic liquids (ILs) have been widely studied for their potential to replace conventional HDS. However, while their success has been demonstrated at the laboratory level, studies on industrial-scale feasibility and their integration into process simulators such as Aspen Plus are limited. In this work, 26 commercially available ILs have been screened using COSMO-based models and Aspen Plus for the desulfurization of diesel fuel and several possible process configurations have been examined. In particular, the challenge of ionic liquid regeneration, which has largely been ignored in the literature, has also been addressed and several potential regeneration methods have been proposed including extractive regeneration (E-RE) and stripping regeneration using nitrogen and air as stripping media (S-RE). The results indicate that, among the 26 ILs studied, 1-butyl-3-methylimidazolium thiocyanate is the most promising as a solvent for extractive desulfurization (EDS), E-RE, and S-RE. E-RE was found to be more effective for the removal of dibenzothiophene (DBT), while S-RE is more suited to the removal of thiophene and benzothiophene (BT). As a result, an optimized diesel desulfurization process using 1-butyl-3-methylimidazolium thiocyanate has been proposed that achieves ULSD with <10 ppm total sulfur in simulation studies, with complete recycling of the IL and minimal loss of the model diesel.



1. INTRODUCTION

During the burning of petroleum-based fuels, sulfur compounds undergo combustion, forming sulfur dioxide (SO₂), which, when present in the atmosphere, leads to adverse health and environmental effects. For example, SO₂ has been attributed to various respiratory complications in humans.¹ Furthermore, it reacts with water, forming sulfuric acid, which contributes to acid rain, leading to acidification of waterways, deforestation, and corrosion of building structures.² In 2016, strict environmental and industrial standards to reduce the sulfur content in diesel to 15 ppm were issued by regulating bodies around the world, such as the U.S. EPA and ASTM.³ In the European Union, where specifications allowed a sulfur content of 2000 ppm in the 1990s, the limit was drastically reduced in 2009 to 10 ppm.⁴ As a result of these regulations, the focus on improving the desulfurization technologies employed in refineries has intensified.

In today's refineries, hydrotreatment is the conventional method used for the removal of sulfur and its derivatives via the process commonly referred to as hydrodesulfurization (HDS).⁵ It is a catalytic process that uses cobalt molybdenum or nickel molybdenum catalysts to convert elemental sulfur and organo-

sulfur compounds, such as thiophene (C₄H₄S), benzothiophene (C₈H₆S) and dibenzothiophene (C₁₂H₈S), to hydrogen sulfide (H₂S) via reaction with hydrogen.⁶ The key disadvantages of the existing HDS method for the production of ultralow sulfur diesel (ULSD) are the requirement for harsh operating conditions such as elevated temperatures and pressures in the ranges of 290–455 °C and 10–207 bar, respectively,^{7,8} and the consumption of large amounts of hydrogen. In addition, while the process can efficiently remove less complex sulfur compounds, such as sulfides, thiols, and thiophenes, it is relatively ineffective in the removal of sterically hindered compounds such as benzothiophene, dibenzothiophene, and their derivatives. The difficulty in the removal of organosulfur compounds stems from their sterically hindered structure;

Received: March 23, 2023

Accepted: July 5, 2023

Published: August 8, 2023



saturation is required to break their aromaticity and allow the molecule to twist so that the catalyst surface may access the sulfur atom and remove it.^{9,10} As a result of these drawbacks, several alternative and complementary processes to the conventional HDS have been proposed to achieve the desired levels of sulfur with the lowest possible energy demands, capital, and operating costs.

Ionic liquids (ILs) have been widely researched in efforts to develop industrial processes that can complement or replace the conventional HDS. ILs are green organic solvents that are composed of ions and exist in a liquid state at moderately low/ambient temperatures. The most significant quality of ILs is the possibility to tailor them to meet certain tasks. In addition, they possess several distinguishing properties that make them excellent alternatives to several solvents and catalysts.^{11,12} Their unique properties, combined with the possibility of recycling and regeneration, have generated significant interest from academia and, more recently, industry.¹³

Polar organic solvents, such as *N,N*-dimethylformamide (DMF), dimethyl sulfoxide (DMSO), and sulfolane (SULF), have been reported in the literature for extractive desulfurization. Hanson et al.¹⁴ highlighted the selective solvent capabilities of DMF, DMSO, and SULF for thiophene removal. Similarly, Zhang et al.¹⁵ conducted liquid–liquid equilibrium (LLE) experiments involving thiophene, octane, and DMSO and found that DMSO exhibited a high selectivity of 1573.48 at 40 °C when the thiophene content in the raffinate phase reached 1.04 wt %. Tao et al.¹⁶ measured the solubility of dibenzothiophene in nine different organic solvents within a temperature range of 9.6–68 °C and found that DMF displayed significant solubility toward dibenzothiophene. Furthermore, Saha et al.¹⁷ conducted an investigation on the extraction of thiophene from model fuel using various solvents, namely, *N*-methyl-2-pyrrolidone (NMP), DMF, and ethylene glycol (EG), under atmospheric pressure conditions. Their findings indicate that NMP exhibited the highest efficacy, achieving a remarkable 98% removal of thiophene within a 1 h timeframe. Additionally, Shekaari et al.¹⁸ analyzed LLE data for the extraction of *n*-hexane and thiophene using *N*-formylmorpholine (NFM), sulfolane (SULF), and diglycolamine (DGA) as extractants. Their findings revealed that the average distribution coefficients at 30 °C were 0.67, 0.79, and 0.96 for NFM, SULF, and DGA, respectively. Moreover, when the thiophene content in the raffinate phase reached approx. 0.1 (molar fraction), the corresponding selectivity maxima were 27.39, 47.42, and 51.83 for NFM, SULF, and DGA, respectively.

When comparing ionic liquids (ILs) to the organic solvents, such as DMF, DMSO, and SULF, several notable advantages of ILs emerge. First, ILs offer the potential for higher selectivity and distribution coefficients compared to organic solvents. ILs can be custom-designed and tailored for specific applications, which highlights their ability to achieve even greater selectivity and distribution coefficients, leading to improved desulfurization efficiency. Additionally, alternative solvents have been investigated, such as deep eutectic solvents (DES) and poly(ethylene glycol) (PEG). DESs share similarities with ILs but have some notable advantages, including easy synthesis, low toxicity, and low cost. However, DESs have shown lower desulfurization efficiency compared to ILs.^{19,20} PEG has also been studied for desulfurization but has limited use due to its lower efficiency and selectivity, particularly for high-molecular-weight sulfur compounds like dibenzothiophene (DBT).²¹ Although PEG has advantages such as low toxicity, low cost, and ease of synthesis

compared to ILs, ILs remain the preferred choice due to their superior desulfurization performance. Studies have shown that using PEG as a modifier with ILs can enhance desulfurization performance by increasing the electrostatic $n-\pi$ interactions between ILs and sulfur compounds while also reducing the toxicity and increasing the biodegradability of ILs.^{22,23}

Mixed solvents provide a notable advantage by harnessing the strengths of two solvents and allowing for enhanced extraction performance through the adjustment of the solvent mixing ratio. This unique characteristic enables researchers to optimize the extraction process by leveraging the complementary properties of different solvents. Despite the potential benefits, there are few studies focusing on the use of mixed solvents in extractive desulfurization of fuel oil. Yan et al.²⁴ highlighted the application and efficacy of mixed solvents in this field. In summary, when comparing ionic liquids (ILs) to organic solvents like DMF, DMSO, and SULF, ILs offer unique advantages in terms of selectivity, distribution coefficients, negligible vapor pressure, and the ability to be custom-designed. However, alternative solvents such as DES and PEG have also been studied, each with its own advantages and limitations. Ionic liquids stand out as promising options for desulfurization due to their selective removal of sulfur compounds, potential for complete regeneration, and nonvolatile nature, which makes them environmentally friendly. While the cost of ILs may be higher than some alternative solvents, their potential for designability, complete regeneration, and reuse can potentially make them more viable in the long run.

Various researchers have demonstrated the use of ILs in desulfurization of diesel as a promising and an environmentally benign technology.²⁵ Several techniques have been investigated, including extractive desulfurization (EDS), oxidative desulfurization (ODS), combined extractive and oxidative desulfurization (ECODS), and desulfurization using immobilized ILs.^{26–33} The main factors that influence the results obtained from each technique include the length of the alkyl chain of the IL cation, the type of cation and anion, temperature, pressure, and time. What all these techniques have in common is their superior ability to extract high-molecular-weight sulfur compounds, such as BT and DBT, at mild operating conditions relative to those of conventional HDS. Dharaskar et al.³⁴ used 1-butyl-3-methylimidazolium thiocyanate [C_4MIM][SCN] as an extractant, resulting in DBT removal as high as 86.5% under a mild temperature of 30 °C. DBT removal of 85.6% was also recorded by Zolotareva et al. using trihexyl(tetradecyl)phosphonium tetrafluoroborate [THTDP][BF₄] under the same operating conditions.²⁸ Furthermore, using the same method, DBT removal of 83.94% using the trialkylamine-based protic ionic liquid [TDA][SA] was also noted by Wang et al. at 25 °C.³⁵ Many studies have demonstrated that the pressure required in EDS is, ideally, atmospheric. The ideal temperature required for EDS is in the range of 25–40 °C, beyond which sulfur removal becomes limited.^{27,32,34,35} Generally, extraction capacity should be measured at equilibrium. Increasing the length of the alkyl chain on the cation has been reported to cause an increase in the desulfurization efficiency.³⁸ On the other hand, Fonseca et al.³⁹ noted that there was no improvement in sulfur recovery when the cation alkyl chain was increased using EDS. Despite the numerous desirable properties that ILs possess, their application still requires extensive research and development to enable the industrial scale-up of IL-based processes. This is due to the several challenges that are yet to be overcome, including the development of appropriate IL recovery and regeneration

methods to conceptualize an optimized industrial-scale process, difficulty of integrating IL-based processes into simulation programs, the lack of appropriate waste disposal routes of spent IL, and the extent of their environmental impact. While desulfurization processes using ionic liquids have been widely researched on the laboratory scale, few have comprehensively studied the feasibility of implementing ionic liquid-based desulfurization on an industrial scale.

To date, ILs have not been included in component databases of widely known process simulators such as Aspen HYSYS and Aspen Plus due to the lack of availability of physical and thermodynamic model parameters for ILs and their mixtures. Thermodynamic models such as nonrandom two-liquid (NRTL),⁴⁰ universal quasichemical (UNIQUAC),⁴¹ functional group activity coefficients (UNIFACs),⁴² and conductor-like screening model for real solvents (COSMO-RS and COSMO-SAC)^{41,42} are the most widely used predictive models. The COSMO-RS is first developed by extension of a dielectric continuum-solvation model to liquid-phase thermodynamics, and the COSMO-SAC (where SAC represents a segment activity coefficient) is a modified version of the COSMO-RS.⁴⁵ The COSMO-RS model has general parameters and element-specific parameters, while the COSMO-SAC model has general parameters but also uses some of the COSMO-RS parameters, such as the element-specific parameters. NRTL and UNIQUAC are the most accurate but are limited to those systems containing pairs of components whose phase behavior has been studied experimentally, and their pairwise interaction coefficients are available. UNIFAC, the group contribution-based predictive activity coefficient model, can be applied to a wider array of IL-containing systems since it is based on interaction between smaller functional groups rather than whole species. However, there are still many binary interaction parameters for functional group pairs missing, which limits the breadth of applicability of this model. A promising alternative when binary interaction parameters are not available is the COSMO-based approach, which uses quantum calculation as a basis for predicting phase equilibria. As a result, this method can be applied to any system without the need for binary interaction parameters regressed from experimental data.

The aim of this work is to investigate the technical feasibility of implementing ionic liquid-based desulfurization on an industrial scale in oil refineries to complement or replace the existing HDS. Several possible process configurations have been conceptualized and compared using the COSMO-SAC thermodynamic model within the Aspen Plus process simulation package. In particular, the challenge of ionic liquid regeneration, which has largely been ignored in the literature, has been addressed, and several potential regeneration methods have been compared using applicable simulation tools.

2. METHODOLOGY

2.1. Quantum and Statistical Thermodynamic Calculations.

The TURBOMOLE suite (TmoleX)⁴⁶ and the program package COSMOthermX⁴⁷ were used, respectively, in all of the quantum chemical and COSMO calculations. The COSMOthermX calculations use the implicit def-TZVP parametrization, and the quantum mechanical modeling method is chosen to be the density functional theory (DFT) and the BP86 functional was used to optimize the geometry.⁴⁸ After optimization, a COSMO file containing the ideal screening charges on the molecular surface was computed for each component. The components included *n*-hexadecane as the

model diesel, thiophene, BT, DBT, hexane, nitrogen, air, and several IL cations and anions each with their own COSMO file. *N*-hexadecane was chosen to represent diesel for simulation purposes in this work due to its relatively high concentration in typical diesel and the similarity of its physical and chemical properties to those of diesel.⁴⁹ The COSMO files were imported into COSMOthermX, and the sigma profiles were generated for each component. A sigma profile can be defined as the probability distribution of a molecular surface segment having a certain charge density. Once the extraction process was simulated using a set of 26 commercially available ILs, the extraction efficiencies were validated against results obtained from the literature. The multicomponent liquid–liquid equilibrium calculations were carried out based on a model diesel feed containing 10,500 ppm total sulfur, which falls within the range found in some of the UAE's well-known crude oil fields as shown in Table 1. Diesel is a fraction of crude oil after treatment; as such, the sulfur content of crude oil can serve as a reasonable benchmark for the sulfur content of the diesel fraction prior to treatment.

Table 1. Sulfur Content of Crude Oil from Major Oil Fields in the UAE⁵⁰

oil field	total PPM sulfur
Murban crude oil	7,780
Das crude oil	11,400
Upper Zakum crude oil	19,500

The model diesel was assumed to contain three model sulfur compounds, thiophene, benzothiophene (BT), and dibenzothiophene (DBT), according to the compositions shown in Table 2.

Table 2. Composition of Model Diesel with a Total Sulfur Content of 10,500 ppm

component	PPM sulfur	mass fraction	number of moles	mole fraction
<i>n</i> -hexadecane		0.9583	4.2321×10^{-3}	0.9271
thiophene	1,648.5	0.0043	5.1411×10^{-5}	0.0114
benzothiophene	8,671.5	0.0363	2.7044×10^{-4}	0.0602
dibenzothiophene	180	0.0010	5.6136×10^{-6}	0.0012
total	10,500	1	4.5595×10^{-3}	1

2.2. Ionic Liquid Database Creation and Integration into Aspen Plus.

A database of commercially available ILs was created for incorporation into the Aspen Plus simulation. It consisted of 26 unique ILs, composed of 14 different cations and 15 different anions. The IL components were introduced into Aspen Properties as conventional components using information obtained via the COSMO calculations along with several calculated parameters and data. The COSMO-SAC thermodynamic model was selected because it allows the screening of a wide range of ILs for which the binary parameters of other models do not exist. For each component, it has six input parameters. CSACVL is the component COSMO volume parameter, obtained from the COSMO calculation. SGPRF1 to SGPRF5 are five component sigma profile parameters; each can store up to 12 points of sigma profile values, representing the full probability distribution. The sigma profile parameters were obtained from COSMOtherm after importing the COSMO files for each component. For ILs, each ion was simulated

Table 3. Abbreviations and Characteristic IDs of Ionic Liquids

IL ID	ionic liquid	IL ID	ionic liquid
01	trihexyltetradecyl phosphonium bromide	14	1-ethyl-3-methylimidazolium bis(trifluoromethylsulfonyl)imide
02	trihexyltetradecyl phosphonium chloride	15	1-butyl-3-methylimidazolium trifluoromethanesulfonate
03	1-dodecyl-3-methylimidazolium bis(trifluoromethylsulfonyl)imide	16	1-ethyl-3-methylimidazolium tetrafluoroborate
04	1-ethyl-3-methylimidazolium diethyl phosphate	17	1-butyl-3-methylimidazolium thiocyanate
05	1-butyl-3-methylimidazolium chloride	18	1-butyl-3-methylimidazolium hexafluorophosphate
06	1-decyl-3-methylimidazolium chloride	19	1-butyl-3-methylimidazolium tetrafluoroborate
07	1-dodecyl-3-methylimidazolium iodide	20	1-ethyl-pyridinium tetrafluoroborate
08	1-decyl-3-methylimidazolium tetrafluoroborate	21	1-ethyl-3-methylimidazolium hexafluorophosphate
09	1-butyl-3-methylimidazolium bromide	22	1-butyl-3-methylimidazolium hydrogen sulfate
10	1-butyl-3-methylimidazolium bis(trifluoromethylsulfonyl)imide	23	1-butyl-3-methylimidazolium nitrate
11	butyltrimethylammonium bis(trifluoromethylsulfonyl)imide	24	1-butyl-3-methylimidazolium dicyanamide
12	1-butyl-3-methylimidazolium iodide	25	1-butyl-1-methylpyrrolidinium dicyanamide
13	choline acetate	26	1-ethyl-3-methyl-imidazolium thiocyanate

Table 4. Model Equations for Estimation of NBP, Densities, Critical Properties, Ideal Gas Heat Capacity Coefficients (CPIG), and Liquid Heat Capacity (CPLDIP)^a

property	model equation	ref
normal boiling point T_b (K)	$T_b = 198.2 + \sum n\Delta T_b$ (1)	51
critical temperature T_c (K)	$T_c = \frac{T_b}{A + B \sum n\Delta T_c - (\sum n\Delta T_c)^2}$ (2) where $A = 0.5703$, $B = 1.0121$	51
critical pressure P_c (bar)	$P_c = \frac{MW}{[C + \sum n\Delta P_c]}$ (3) where $C = 0.2573$, $MW =$ molecular weight in g/mol	51
critical volume V_c (cm ³ /mol)	$V_c = D + \sum n\Delta V_c$ (4) where $D = 6.75$	51
density model	$\rho = \frac{A}{B} + \left(\frac{2}{7} \times \frac{A \ln B}{B} \times \frac{T - T_b}{T_c - T_b} \right)$ (5) where $A = 0.3411 + \frac{2.0443 \times MW}{V_c}$, $B = \left(\frac{0.5386}{V_c} + \frac{0.0393}{MW} \right) \times V_c^{1.0476}$	53
acentric factor ω	$\omega = \frac{(T_b - 43)(T_c - 43)}{(T_c - T_b)(0.7T_c - 43)} \times \log\left(\frac{P_c}{P_b}\right) - \frac{(T_c - 43)}{(T_c - T_b)} \times \log\left(\frac{P_c}{P_b}\right) + \log\left(\frac{P_c}{P_b}\right) - 1$ (6) where $P_b = 1.013$ bar	51
CPIG parameters	$C_1 = (nC_{pAk} - 37.93) \times 1000$ (7.1) $C_2 = (nC_{pBk} - 37.93) \times 1000$ (7.2) $C_3 = (nC_{pCk} - 37.93) \times 1000$ (7.3) $C_4 = (nC_{pDk} - 37.93) \times 1000$ (7.4) where C_{pAk} , C_{pBk} , C_{pCk} and C_{pDk} are group contribution parameters	52
ideal gas heat capacity $C_p^o(T)$	$C_p^o = \left[\sum nC_{pAk} - 37.93 \right] + \left[\sum nC_{pBk} + 0.210 \right] T + \left[\sum nC_{pCk} - (3.91 \times 10^{-4}) \right] T^2 + \left[\sum nC_{pAk} + (2.06 \times 10^{-7}) \right] T^3$ (8)	52
liquid heat capacity $\frac{C_p^r}{R} = \frac{C_p - C_p^o}{R}$	$\frac{C_p^r}{R} = 1.586 + \frac{0.49}{1 - T_r} + \omega \left[4.2775 + \frac{6.3(1 - T_r)^{1/3}}{T_r} + \frac{0.4355}{1 - T_r} \right]$ (9) where T_r is reduced temperature	52

^aNB: n is the number of groups of type k in the molecule.

individually, and the parameters for the IL were obtained via the addition of the COSMO volume and sigma profile parameters of

the respective cation and anion. A similar approach was used by Ferro et al.,⁴⁸ and the simulations were performed without

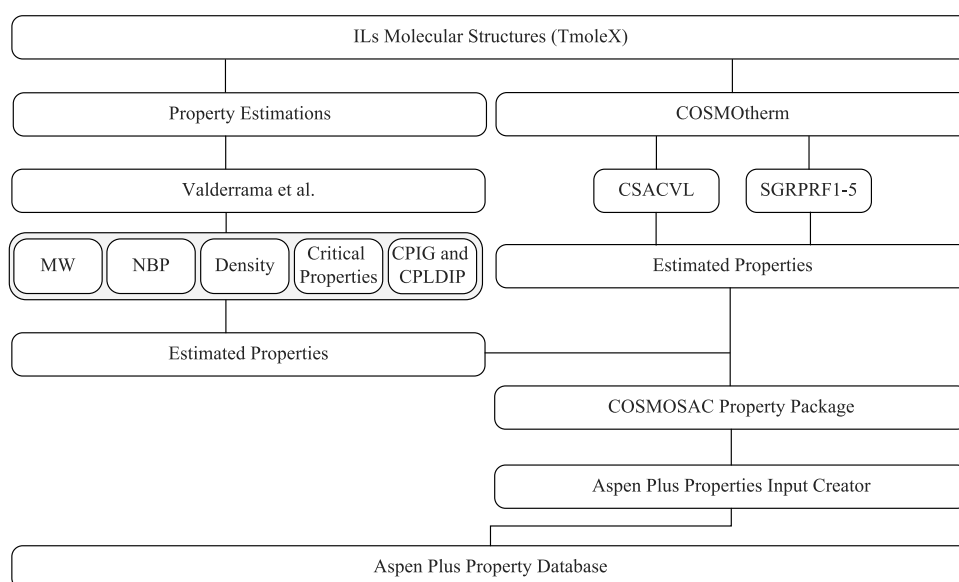


Figure 1. Information flow of the methodology used in database creation and integration of ILs into Aspen Plus.

Table 5. Output of Multicomponent Two-Phase Equilibrium Using COSMOtherm^a

	compound/ion	model diesel (mole fraction)		IL phase (mole fraction)	
		initial	final	initial	final
1	1-butyl-3-methyl-imidazolium		0.0001	0.5000	0.4797
2	bistrifluoromethylsulfonamide		0.0001	0.5000	0.4797
3	<i>N</i> -hexadecane	0.9271	0.9674		0.0002
4	thiophene	0.0114	0.0051		0.0063
5	BT	0.0602	0.0267		0.0335
6	DBT	0.0012	0.0007		0.0006

^aCondition settings: $T = 25$ °C. Equimolar amounts of the cation and anion were input into the IL phase.

problems of consistency related to IL incorporation as user-defined ionic pairs. In addition to the COSMO-SAC parameters, each user-defined component in Aspen Plus requires molecular weight (M_w), normal boiling point (NBP), density, critical properties, ideal gas heat capacity coefficients (CPIGs), and liquid heat capacity (CPLDIP) to be precalculated and added. NBP, critical properties, and acentric factor were estimated for each IL using the Valderrama et al. method,⁵¹ while the CPIG values were estimated using the Ge et al. method.⁵² The IUPAC names of ILs are usually long and cannot be accommodated in the 8-character format used by Aspen Plus to identify the components. As a result, abbreviations were used to designate them in the creation of the database. Each IL included in the current database has its own characteristic ID ranging from IL01-IL26 as shown in Table 3. The database can be found in the Supporting Information.

Valderrama group contribution method⁵¹ was used to calculate the contribution toward the normal boiling point (NBP) and the critical properties including critical temperature, pressure, and volume for each cation and anion under study, and the value for each IL was determined via the sum of the contributions of the relevant cation/anion pair. The acentric factors of the ILs were calculated using Rudkin's equation using the estimated critical temperatures, critical pressures, and normal boiling points.⁵¹ The densities of the ILs were estimated using the method used by Valderrama and Rojas 2009.⁵³ The Joback group contribution method was used as a predictive tool to calculate the ideal gas heat capacities for ionic liquids. By

applying the principle of corresponding states, the ideal gas heat capacity, along with other thermodynamic properties of the component, was used to estimate the liquid heat capacity at various temperatures.⁵² Table 4 summarizes the model equations used to calculate the above-mentioned properties.

Since ILs have negligible volatility under normal process conditions, the first coefficient of the extended Antoine vapor pressure (PLXANT-1) for all ILs was manually set to be 1×10^{-10} , which ensures that they remain in the liquid phase during simulation. All mentioned properties have been used to create the database, which has been successfully integrated into Aspen Plus. The remaining physical and thermodynamic properties necessary to completely define the IL components were automatically estimated using the API-recommended procedures within Aspen Plus.

Figure 1 shows the information flow of the methodology used in this work to both create the IL component database and specify the COSMO-SAC property model. More details about the Aspen Plus setup and validation can be found in section B of the Supporting Information.

In the absence of available bulk industrial prices for IL, in order to facilitate comparison and screening on the basis of IL cost, the relative price of each IL was calculated by taking the laboratory-scale IL price (Iolitec) and dividing it by the equivalent price of a traditional solvent commonly reported for extractive desulfurization. NMP was selected as the traditional solvent, and the price of a similar quantity and purity from a lab supplier (Sigma-Aldrich) was used. The relative price

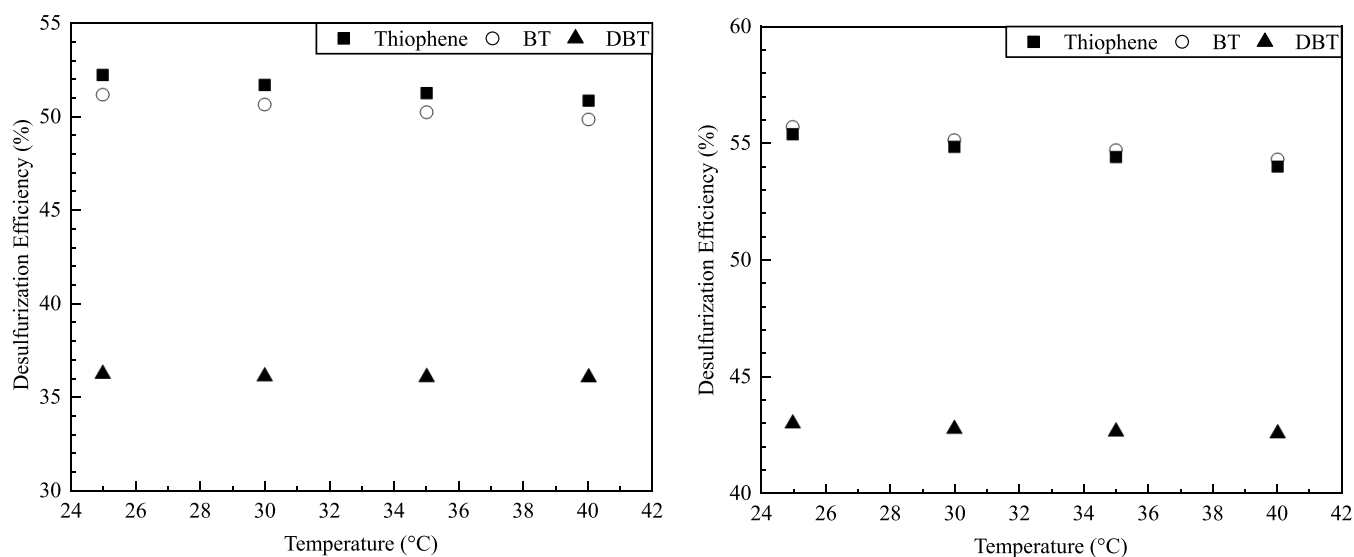


Figure 2. Temperature dependence of thiophene, BT, and DBT removal from model diesel using [C₂MIM] bis(trifluoromethylsulfonyl)imide (left) and [C₄MIM] bis(trifluoromethylsulfonyl)imide (right) as simulated using COSMOtherm.

is included purely to assist in screening between the ILs and is not intended as a basis for a detailed economic analysis of the process.

3. QUANTUM AND STATISTICAL THERMODYNAMIC CALCULATIONS

The COSMO files were imported into COSMOtherm to carry out the liquid–liquid extraction simulation. The converged system thus provides two new phases I (Model diesel phase) and II (IL phase), with all compounds distributed between the two phases according to their thermodynamic equilibrium partition. It can be seen in Table 5 that most of the *n*-hexadecane remains in the model diesel phase and sulfur compounds will move to the IL phase. The same holds for the IL phase, which mainly remains stable, and small amounts of 1-butyl-3-methylimidazolium cation and bis(trifluoromethylsulfonyl)imide anion move to the *n*-hexadecane phase (model diesel).

Based on the calculation output depicted in Table 5, the desulfurization efficiency was calculated using eq 10.

$$DE = \frac{X_{\text{diesel,initial}} - X_{\text{diesel,final}}}{X_{\text{diesel,initial}}} \times 100\% \quad (10)$$

where $X_{\text{diesel,initial}}$ and $X_{\text{diesel,final}}$ are the initial and final model diesel phase mole fractions, respectively. Using eq 10, the desulfurization efficiencies of 1-butyl-3-methylimidazolium bis(trifluoromethylsulfonyl)imide were found to be 55.38, 55.69, and 43.01% for thiophene, BT, and DBT, respectively. The method was repeated for all 26 ILs within this study and has been compared and validated against results obtained from the literature; reference can be made to section A of the Compound Information for the tabulated results. In addition, a database was created showing the other key parameters necessary for the integration of the ILs into Aspen Plus simulations.

4. VALIDATION OF THE THERMODYNAMIC MODEL

To validate the COSMO-based approach for the IL–diesel system, the results obtained from the COSMOtherm liquid–liquid extraction tool were compared against some of the data presented in the literature. For instance, Jha et al.⁵⁴ used trihexyltetradecyl phosphonium chloride IL for the desulfuriza-

tion of diesel using EDS, and their results show that 81.4% DBT was extracted, and using the COSMOtherm approach resulted in 82.65% DBT extraction. Reference can be made to Table S2 in the Supporting Information for the comparison of literature results to those using the COSMOtherm approach for several ILs. The results obtained from the COSMOtherm simulations are within an acceptable limit of agreement with data reported in the literature, with average deviations of 14.89, 13.61, and 17.59% for thiophene, BT, and DBT, respectively. Therefore, it is safe to say that the thermodynamic model used serves as a good screening tool for ranking the desulfurization efficiency of the ILs under study.

4.1. Temperature Dependence. The results obtained from COSMOtherm simulations were compared to observations collected from a literature review. It was reported in a previous study that extraction is mostly favored by mild temperature conditions in the range of 25–70 °C for most ILs. However, care must be taken when setting the temperatures for multicomponent two-phase equilibrium calculations. Since some ILs have relatively high melting points, the extraction temperature should be set higher than the melting point of the chosen IL. If the extraction temperature is below the melting point of the IL, it can lead to the formation of a solid phase, which would cause the extraction process to fail in the real process, while this would not be picked up by the phase equilibria model. Mild temperature conditions are also of importance as they promote lower energy consumption, a key criterion for technoeconomic feasibility. The previous research trends suggest that the extraction efficiency tends to increase with temperature up to a certain point, after which the improvements become less significant or plateau, emphasizing the need for careful temperature optimization to maximize the extraction efficiency. It is worth noting that this trend is not always observed in every case, and there may be other factors that can affect the extraction efficiency of an IL toward sulfur compounds, such as the IL concentration, the type and concentration of cosolvents or additives, and the type and concentration of impurities present in the sample. Varying the extraction temperature using 1-butyl-3-methylimidazolium [C₄MIM] bis(trifluoromethylsulfonyl)imide and 1-ethyl-3-methylimidazolium [C₂MIM] bis(trifluoromethylsulfonyl)-

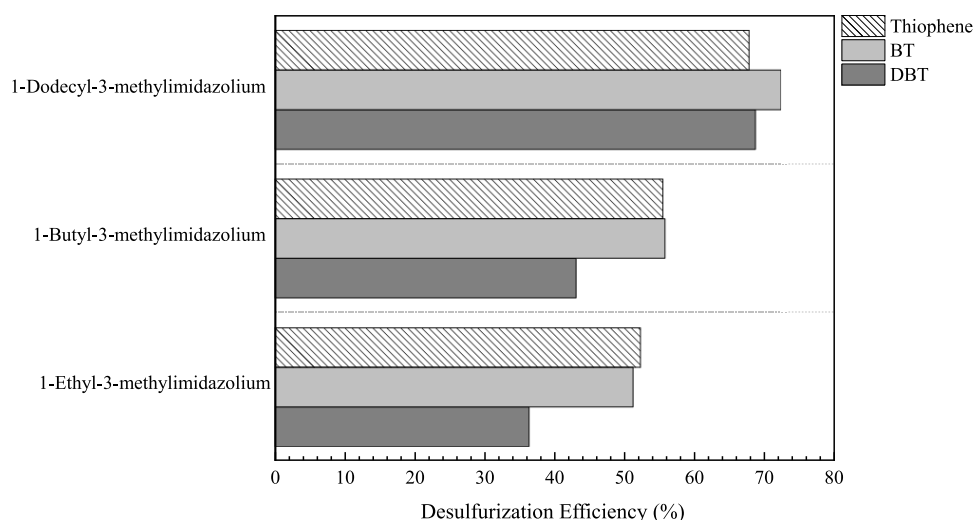


Figure 3. Effect of cation alkyl chain length on the desulfurization efficiency of 1-alkyl-3-methylimidazolium bis(trifluoromethylsulfonyl)imide ILs, as simulated using COSMOtherm.

imide was found to cause a slight decrease in the desulfurization efficiency, which is almost negligible for thiophene, BT, and DBT. This can be seen in Figure 2. Wang et al. experienced a relatively similar result with protic ionic liquids using EDS in which the extraction efficiency of DBT and thiophene increased slightly within 15–25 °C and then began to decrease with the increase of temperature. However, for BT, the extraction efficiency decreased slightly right from the very beginning.³⁵ Furthermore, Dehghani studied the extraction of thiophene from *n*-decane by [C₄MIM] nitrate and [OMIM] nitrate using three different temperatures (15, 25, and 40 °C). In his study, he concluded that the temperature increase showed little to no effect on desulfurization.⁵⁵ The agreement of the results with conclusions from the literature is deemed very important from an industrial point of view because the process can be essentially carried out at ambient temperatures requiring lower energy consumption.

4.2. Length of Cation Alkyl Chain. Extraction simulations using COSMOtherm were performed at 25 °C to verify the effect of cation alkyl chain length on the extraction efficiency. Zhang et al.³⁶ noted that as the length of the alkyl chain increases, the extraction efficiency increases.³⁷ In their study, [C₄MIM][BF₄] demonstrated higher extraction of sulfur components in comparison to [C₂MIM][BF₄]. In this study, Figure 3 shows the effect of increasing the alkyl chain on 1-alkyl-3-methylimidazolium bis(trifluoromethylsulfonyl)imide ILs, and the results match the trend reported in the literature.

4.3. Effect of Anion Type on Desulfurization Efficiency. Varying the anions has also proved to be a contributing factor to the desulfurization efficiency. Results obtained from the simulations agree with the results reported in the literature. For instance, the results of the extraction efficiencies of [C₄MIM] hexafluorophosphate and tetrafluoroborate are in agreement with those of Zhang et al.'s study. With [PF₆]⁻ and [BF₄]⁻ having diameters of 2.4 and 2.2 Å, respectively, [PF₆]⁻ would result in better extraction efficiency by absorbing more of sulfur compounds.³⁶ Moreover, the study conducted by Zhang et al. demonstrated that [C₄MIM][PF₆] exhibited a higher absorption capacity for toluene (model diesel) compared to [C₄MIM][BF₄], which was also supported by the COSMOtherm liquid–liquid extraction simulation. The presence of the [PF₆]⁻ anion resulted in a greater extraction of thiophene, BT,

and DBT, while the addition of hexafluorophosphate led to a lower amount of *n*-hexadecane in phase 1. Consequently, this implies that a larger proportion of *n*-hexadecane was present in phase 2 due to the extraction using the [PF₆]⁻ anion. Therefore, in line with the findings of Zhang et al., it can be concluded that the utilization of [C₄MIM][PF₆] as an extractant leads to a lower extraction efficiency compared to [C₄MIM][BF₄], indicating that [BF₄]⁻ is a more favorable anion option for sulfur removal. Results obtained using COSMOtherm are summarized in Table 6.

Table 6. Extraction Efficiency of Hexafluorophosphate versus Tetrafluoroborate Anions in [C₄MIM]-Based Ionic Liquids

cation	anion	extraction temperature (°C)	extraction efficiency		
			thiophene (%)	BT (%)	DBT (%)
C ₄ MIM	PF ₆	25	40.33	36.87	19.76
C ₄ MIM	BF ₄	25	37.51	33.73	17.19

Furthermore, the total sulfur removal was analyzed using ILs with different anions and the [C₄MIM] cation. As shown in Figure 4, the results showed that the chloride anion achieved the highest total sulfur removal followed by the bis(trifluoromethylsulfonyl)imide anion.

4.4. Ionic Liquid Selection and Agreement with Literature Results. It is desirable that the ionic liquid with the highest extraction efficiency is selected. However, other important criteria for the techno-economic analysis include IL availability and cost. All ILs considered in this study are commercially available. Pyridinium-, ammonium-, and imidazolium-based ILs proved to be very promising extractants for EDS; however, they are relatively expensive, so cheaper phosphonium ionic liquids can replace them.²⁸ Trihexyltetradecyl phosphonium chloride has several advantages in comparison to all 26 ILs that were under study: it is the cheapest IL, showed the highest extraction, and its desulfurization efficiency is in good agreement with literature results; however, this IL has high viscosity, which may be an issue in industrial processes due to the lower mass transfer.

Based on the average deviation between the results obtained from the COSMOtherm simulations and the literature as

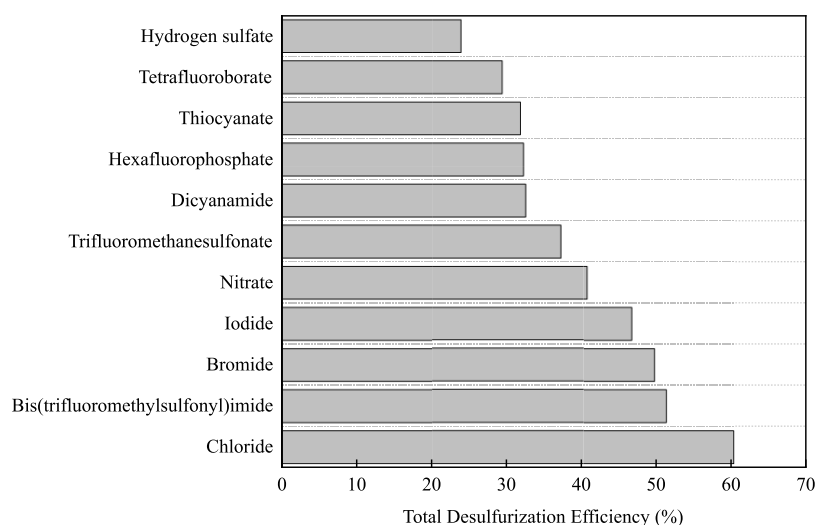


Figure 4. Total sulfur removal efficiencies of [C₄MIM]-based ILs with different anions.

tabulated in Table S2, section A of the supporting information, it can be concluded that the COSMO-based approach is a reasonably reliable thermodynamic model for further process analysis within our Aspen Plus simulations. Following the creation of the database via the highlighted methodology in Section 2.2, the simulations of the proposed configurations using COSMO-SAC property in Aspen Plus were carried out.

5. CONCEPTUALIZATION OF PROCESS CONFIGURATIONS

Extractive desulfurization using ILs has proven to be a possible alternative to HDS on an experimental basis due to its milder operating conditions and efficient removal of high-*M_w* sulfur compounds such as BT and DBT. *N*-hexadecane was chosen to represent diesel for simulation purposes in this work due to its relatively high concentration in typical diesel and the similarity of its physical and chemical properties to those of diesel.³⁵ EDS was chosen as a first step to achieve the desired level of diesel desulfurization, followed by IL regeneration. The first configuration was using EDS combined with IL regeneration using *n*-hexane as an extractant. *N*-hexane was used due to its attributes such as simple recovery via distillation, nonpolar nature, and low latent heat of vaporization (330 kJ/kg).⁴² The second configuration was using EDS combined with regeneration using nitrogen or air stripping. Based on the results obtained from both configurations, a third combined and optimized configuration has been proposed. This was necessary to achieve ULSD, complete removal of thiophene, BT, and DBT from the spent IL stream without imposing contaminants such as *n*-hexane and with minimum loss of *n*-hexadecane (diesel).

6. ASPEN PLUS SIMULATION RESULTS

6.1. Aspen Plus Setup and Validation of Results. Two different implementations of the COSMO-based thermodynamic approach, COSMO-RS and COSMO-SAC, are available in Aspen Plus. Each is specified using a different option code. The option codes can be selected by the user through the option codes in the γ calculations when the COSMO-SAC property model is selected (Properties → Methods → Selected Methods). Option codes 1 and 2 correspond, respectively, to two different models and COSMO equations as seen in Table 7.

Table 7. COSMO-SAC Property Model Submodels

option code	model
COSMO-SAC option code 1 (OC1)	COSMO-SAC model proposed by Lin and Sandler ⁴⁴
COSMO-SAC option code 2 (OC2)	COSMO-RS model proposed by Klant ⁴³

Before carrying on with desulfurization and regeneration simulations, a preliminary check was carried out to verify which model is best suited for further use based on its agreement with the results obtained from COSMOtherm simulations and the results reported in the literature. To perform this preliminary check, several simulations were carried out using a simple decanter to mimic the liquid–liquid extraction simulation performed in COSMOtherm. OC1 demonstrated closer results to literature findings in comparison to OC2. As a result, OC1 was chosen to carry on with the rest of the simulations. The preliminary check results for the COSMO-SAC property model submodels are summarized in Table S3 in the Supporting Information. Once the simulation setup and the validation of results against results reported in the literature are completed, the appropriate property submodel is selected accordingly.

6.2. Configuration 1: EDS followed by Regeneration through Extraction. In the conducted research, a diesel feed with 10,500 ppm sulfur was employed, with specific mole fractions assigned to *n*-hexadecane, thiophene, BT, and DBT (0.9271, 0.0114, 0.0602, and 0.0012, respectively). Unless otherwise specified, an equimolar amount of IL was fed relative to the model diesel feed rate. The IL is fed at the top of the extraction column (EDS) because it has a higher density than the model diesel, while the latter was fed from the bottom. The extraction column was operated adiabatically at atmospheric pressure, at 25 °C for the low-melting-point ILs and at 100 °C for the high-melting-point ILs. The PFD of this arrangement is shown in Figure 5.

Following the same arrangement, extractive desulfurization using ILs was carried out for all 26 ILs (19 low-melting-point ILs and 7 high-melting-point ILs) to evaluate the desulfurization efficiency of the ILs under study. The mass fractions of the diesel product were used to calculate the remaining PPM sulfur after varying the number of extraction stages. The bottom product contains the IL and the extracted sulfur compounds that is to be

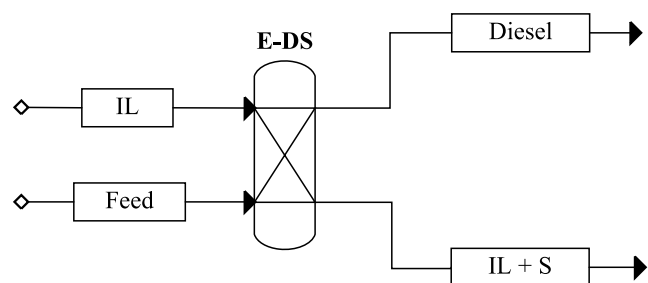


Figure 5. Extractive desulfurization PFD.

further processed in a regeneration unit to regenerate and recycle the ILs.

The extractive regeneration was carried out using *n*-hexane as an extractant for its attributes such as simple recovery, nonpolar nature, low latent heat of vaporization (330 kJ/kg), high selectivity toward sulfur compounds, and low miscibility with ILs. The extractive regeneration works in the following manner. The bottom product of the extractive desulfurization column (EDS) is fed into an extractive regeneration (E-RE) column operated at 25 °C. It is important to maintain the regeneration column at a temperature that is below the boiling point temperature of *n*-hexane (69 °C) to avoid the need for high pressures to maintain the liquid phase. If the temperature in the regeneration column is above the boiling point of *n*-hexane (69 °C), then *n*-hexane will vaporize along with other components, making it difficult to separate from the other components. This could result in the need for higher pressures to maintain the liquid phase and achieve the desired separation, which could be expensive. In the case where high-melting-point ILs were used, the extractive desulfurization is carried out at 100 °C; a cooler is therefore added in between the two extraction columns to cool the feed of the extractive regeneration column. The PFD for the two arrangements can be seen in Figure 6.

6.2.1. Extractive Desulfurization Results of ILs. The extractive desulfurization simulation was carried out for 19 low-melting-point ILs at 25 °C. As the number of stages increased, the sulfur content of the treated diesel decreased for

all ILs under study, which is the expected trend. The same procedure was repeated for the seven remaining high-melting-point ILs at 100 °C, and the results are depicted in Table 8. However, the performance of this configuration is assessed not solely on the least amount of sulfur present in the treated diesel. Other criteria such as relative IL cost, amount of *n*-hexadecane (diesel) lost, amount of solvent left in the recycle stream, and amount of IL lost during the regeneration stage are all of importance in the selection of the most promising ILs. For this purpose, the selection of the most promising ILs and the elimination process will be discussed in the following section.

6.2.2. Extractive Regeneration Results of ILs. All 19 low-melting-point and 7 high-melting-point ILs were simulated using extractive desulfurization and extractive regeneration using *n*-hexane. Some ILs were subsequently eliminated based on their stability, sulfur extraction efficiencies, amount of *n*-hexadecane lost, amount of *n*-hexane present in the recycle stream, and IL loss during the regeneration process. For instance, IL18 and IL21 were eliminated due to stability issues that arise because they contain the hexafluorophosphate anion, which is prone to hydrolysis in the presence of water to form hydrofluoric acid, a byproduct that can be problematic in terms of corrosion.⁵⁶ More than 2000 ppm sulfur was still remaining after three stages of extraction with IL05, IL06, IL09, IL12, IL20, IL22, and IL26; hence, they were eliminated due to their poor sulfur extraction abilities.

Furthermore, IL01-04, IL07, IL08, IL10, IL11, IL13, and IL25 contained more than 2000 kg/h of hexane in the recycle stream, which would contaminate the fuel product, interfere with the desulfurization efficiency, and result in poor extraction. Lastly, since recovering the ILs during the regeneration process is of great importance, ILs that displayed more than 2 kg/h loss of IL were eliminated, namely, IL24. The elimination process is further documented in Table 8. Hence, out of 26 ILs, only 6 ILs were chosen to be the most promising for further analysis using this configuration, namely, IL14, IL15, IL16, IL17, IL19, and IL23. The performance of these six ILs was analyzed by varying the desulfurization extraction stages and observing the amount of *n*-hexane present in the recycle stream, amount of IL present

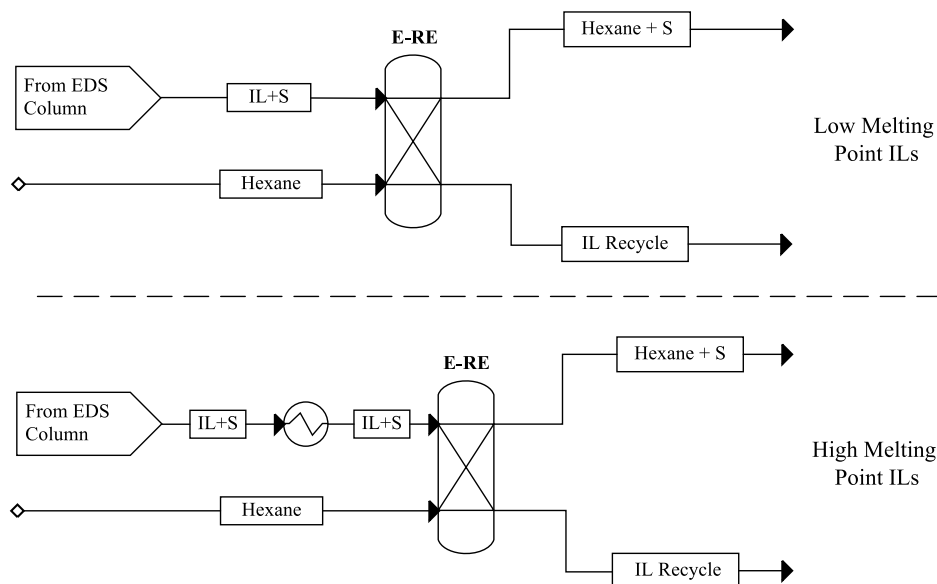


Figure 6. Extractive regeneration PFD.

Table 8. Elimination of ILs Based on Criteria for Extractive Regeneration

IL	Total PPM Sulfur		Post Extractive Regeneration (3 Stages) Recycle Stream (kg/hr)			Relative Price (\$/\$)
	3 Stages	4 Stages	Hexane	IL	IL loss	
IL01	365	286	30,903	202,915	43	15
IL02	343	268	30,875	186,937	19	12
IL03	1,057	838	30,396	191,357	16	53
IL04	601	479	19,133	95,136	0	22
IL08	1,210	772	5,223	111,668	1	40
IL10	1,097	498	4,520	150,973	2	24
IL11	869	454	4,214	142,686	11	31
IL12	4,334	14	6	0	95,806	32
IL14	777	276	1,660	140,874	2	22
IL15	854	359	1,542	103,786	0	27
IL16	1,104	834	309	71,271	0	29
IL17	1,625	1,088	861	71,030	0	19
IL18	1,049	741	433	102,308	0	14
IL19	1,092	804	457	81,370	0	12
IL22	2,685	2,158	650	85,066	0	30
IL23	744	366	1,645	72,442	0	60
IL24	1,001	244	1,302	74,990	11	34
IL25	95	21	3,799	74,990	1	46
IL26	2,498	774	3,799	77	60,854	23
IL05	3,532	2160.43	6,105	62,883	0	19
IL06	2,026	1623.23	9,029	93,181	0	37
IL07	1,873	-	8,076	136,203	1	102
IL09	4,112	-	3,606	78,885	0	20
IL13	641	353.64	3,124	1	58,758	39
IL20	2,316	1638.04	516	70,189	0	82
IL21	2,242	2152.15	635	92,203	6	33

in the recycle stream, and amount of *n*-hexadecane lost through EDS.

6.2.2.1. Varying the Number of Desulfurization Extraction Stages. For the six shortlisted ILs, the number of desulfurization extraction stages was increased from three stages up to six; the results are shown in Figure 7.

The results for all shortlisted ILs followed the expected trend: as the number of extraction stages increased, the total ppm sulfur decreased; this is because with each extraction stage, more sulfur is removed. The lower the ppm sulfur in the extracted sample, the more effective the IL is at removing sulfur using EDS. However, the performance of the configurations in this study is assessed as a whole. Therefore, other criteria such as the amount of extractant (*n*-hexane) and the amount of IL in the recycle stream post regeneration and the amount of *n*-hexadecane (diesel) lost post EDS were considered. The extraction capacity of the sulfur compounds (solubility of sulfur compounds in ILs) is a vital parameter in the EDS process; the capacities are shown in Figure 8. According to the results obtained for the three-stage extraction column, the desulfurization efficiency is on the order of IL23 > IL14 > IL15 > IL19 > IL16 > IL17. The results of the desulfurization efficiencies are relatively in agreement with those

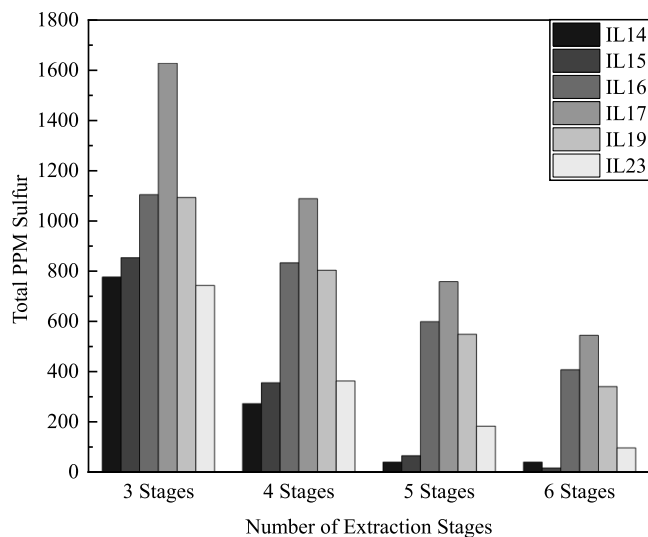


Figure 7. Total ppm sulfur vs extraction stages for the shortlisted ILs.

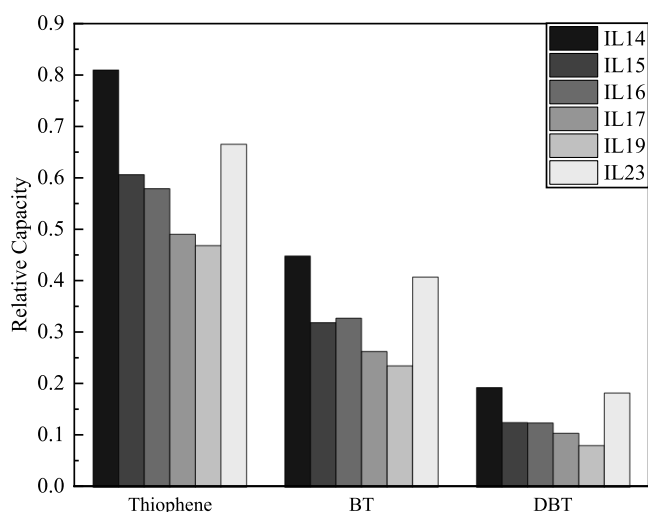


Figure 8. Capacity of ILs toward sulfur components predicted using COSMOtherm.

of the extraction capacity, which implies that ILs with larger extraction capacities result in higher desulfurization efficiency.

It can be seen that IL23 has a higher capacity toward thiophene, BT, and DBT than IL17; hence, it displayed a higher desulfurization efficiency. This can be explained from the micro-level view with the help of sigma profiles. IL17 and 23 have the same cation but different anions. The anions are thiocyanate and nitrate for IL17 and 23, respectively. It can be seen in Figure 9 that the peaks of the anions are located in the polar region, with the nitrate anion having a higher polarity than thiocyanate. High polarity of the cation and anion results in high capacity for sulfur compounds and high desulfurization efficiencies.⁵⁷

6.2.2.2. Amount of *n*-Hexane Present in the Recycle Stream Post Extractive Regeneration. Figure 10 summarizes the results obtained for the six shortlisted ILs in terms of the amount of *n*-hexane (extractant) present in the recycle stream after three extraction stages. It is desired that the amount of extractant (*n*-hexane) be as low as possible to avoid the contamination of the EDS column with the extractant from E-RE.

6.2.2.3. Amount of IL Lost Post Extractive Regeneration. Table 9 summarizes the results obtained for the six shortlisted ILs in terms of amount of IL lost after three extraction stages. Ideally, we require the maximum amount of IL to be present in the recycle stream and not lost with the *n*-hexane and sulfur

component stream during the regeneration. This is necessary as IL costs are high and the maximum amount should be retained for the regeneration to be deemed effective. Negligible losses of ILs were noted for all shortlisted ILs after E-RE.

6.2.2.4. Amount of *n*-Hexadecane Lost through EDS. Figure 11 summarizes the results obtained for the six shortlisted ILs in terms of the amount of *n*-hexadecane (diesel) lost during EDS after three EDS stages. It is desired to maintain low amounts of loss in *n*-hexadecane for this configuration to be efficient. Most of the shortlisted ILs depicted high amounts of *n*-hexadecane loss with the exception of IL17 and IL23. In fact, loss of hydrocarbons is a predominant issue faced with IL-assisted desulfurization and has been documented in various studies, which have suggested that this stems from the mutual solubility of ILs and diesel. It is recommended to screen the ILs based on the ones that display less mutual solubility with *n*-hexadecane via COSMOtherm and to calculate the mutual solubility of the ILs prior to carrying out the simulations.⁵⁸ In our Aspen Plus simulation of EDS, we observed high losses of *n*-hexadecane when using IL14, IL15, IL16, and IL19. The high losses observed can be attributed to several factors. First, the ILs used may have low solubility for *n*-hexadecane, leading to incomplete extraction of sulfur compounds and resulting in high losses of *n*-hexadecane. Additionally, the ILs used may have low selectivity to sulfur compounds, resulting in a lower concentration of sulfur compounds in the IL phase and a higher concentration of *n*-hexadecane in the raffinate phase. Furthermore, the simulation model used may have contributed to the high losses observed. In our simulation, we assumed ideal mixing between the IL and *n*-hexadecane and did not account for any nonideal behavior, such as phase separation or emulsification, which may occur in the actual process. Sensitivity analyses to examine the effects of IL concentration, temperature, and pressure on the loss of *n*-hexadecane can be carried out to investigate the reasons for the observed high losses. In conclusion, the high losses of *n*-hexadecane observed in our Aspen Plus simulation of EDS using the mentioned ILs can be attributed to the properties of the ILs used and the assumptions made in the simulation model. Further studies are needed to optimize the process conditions and IL properties to minimize the loss of *n*-hexadecane and improve the efficiency of the EDS process. As a result, it is recommended to carry out sensitivity studies and assess the solubility of *n*-hexadecane in ILs at early stages to avoid increased separation costs associated with the recovery of dissolved *n*-hexadecane (diesel).

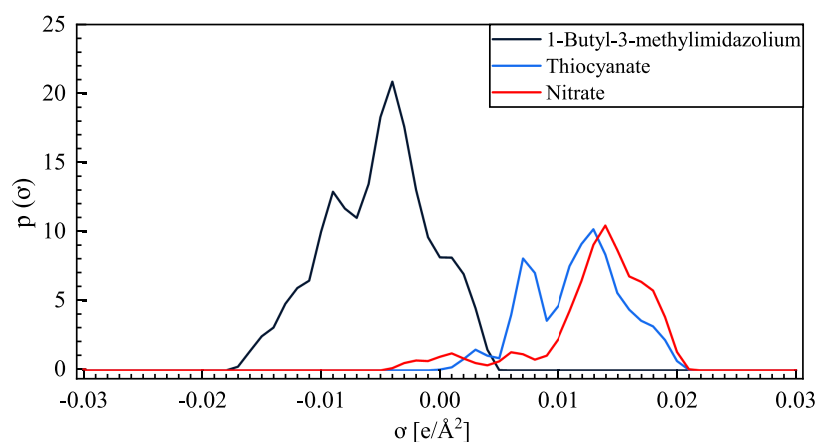


Figure 9. Sigma profiles of IL17 and IL23 for polarity analysis.

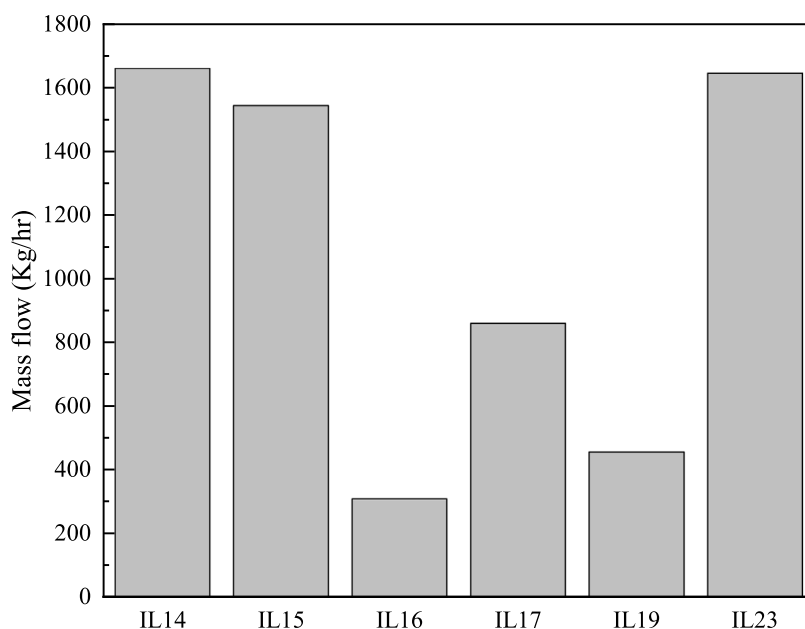


Figure 10. Amount of *n*-hexane present in the recycle stream for the shortlisted ILs.

Table 9. Amount of IL Lost after Extractive Regeneration for the Shortlisted ILs

IL	% IL loss
IL14	1.14×10^{-3}
IL15	2.11×10^{-5}
IL16	1.20×10^{-5}
IL17	4.28×10^{-6}
IL19	1.39×10^{-5}
IL23	9.17×10^{-7}

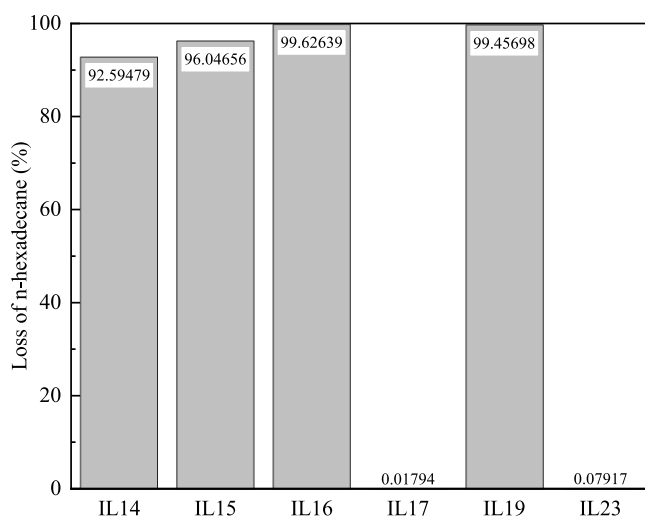


Figure 11. Amount of *n*-hexadecane lost during EDS for the shortlisted ILs.

6.2.3. Process Optimization Results. As can be seen in Tables 10 and 11, each shortlisted IL has its own advantages and disadvantages when employed in this configuration.

Negligible losses of IL were noted for all shortlisted ILs. IL14 and 15 resulted in the least amount of total PPM sulfur after six extraction stages but showed a large amount of *n*-hexane in the recycle stream, and most of the *n*-hexadecane was lost during the EDS. The amount of *n*-hexane in the recycle stream was low for

IL16 and 19; however, the loss of *n*-hexadecane (diesel) was still high and the EDS was not efficient enough. IL23 results were satisfactory in terms of IL loss, *n*-hexadecane loss, and remaining PPM sulfur after six EDS stages. However, the amount of *n*-hexane was high, which may require an additional separation unit to separate the *n*-hexane from the recycled IL leading to an increase in the total cost of this process configuration. IL17 has the potential to be implemented within this configuration as it has shown the best performance with respect to loss of valuable products such as IL and *n*-hexadecane as well as low amounts of *n*-hexane in the recycle stream. However, for IL17, high total PPM sulfur (546.51 ppm) was observed post six stages of EDS; this suggests that the E-RE technique works well with the said IL, but consideration should be given to optimizing the EDS section. This can be done through increasing the number of stages of the EDS column, carrying out several EDS in series, or through coupling it with a different desulfurization method to achieve the desired level of desulfurization. Furthermore, consideration should be given to separate the sulfur compounds from the regeneration solvent (*n*-hexane); this could be done through an additional separation unit such as distillation. Therefore, after several simulations and refinement of results, IL17, namely, 1-butyl-3-methylimidazolium thiocyanate, is the most promising IL for this configuration.

Since the only issue with IL17 (operated at six EDS stages at 25 °C and 1.01325 bar) is that the total ppm sulfur remaining is high, the process was optimized by varying the number of extraction stages to see how many extraction stages are required to obtain ULSD. Increasing the EDS column up to 14 stages resulted in 107.52 ppm total sulfur. To obtain ULSD, it is necessary to operate several extractors in series. Table 12 summarizes the results using several extractors in series, in which all are operated at 25 °C and 1.01325 bar.

In addition, since the extraction favors high operating pressures and temperatures, both parameters were increased to study their effect. Increasing the pressure of the EDS column had little to no effects of the desulfurization efficiency. Furthermore, despite being reported in many literature findings that increasing the temperature will have a positive impact, the

Table 10. Summary of EDS and E-RE Results

shortlisted ILs	E-RE recycle stream (kg/h) (3 E-RE stages)		% IL loss	% loss of <i>n</i> -hexadecane after 3 EDS stages	remaining PPM sulfur after 6 EDS stages
	hexane	IL			
IL14	1,660	140,874	1.14×10^{-3}	92.59	44.85
IL15	1,542	103,786	2.11×10^{-5}	96.05	21.59
IL16	309	71,271	1.20×10^{-5}	99.63	410.40
IL17	861	71,030	4.28×10^{-6}	0.02	546.51
IL19	457	81,370	1.39×10^{-5}	99.46	343.88
IL23	1,645	72,442	9.17×10^{-7}	0.08	100.54

Table 11. Discussion of the Six Shortlisted ILs for Extractive Regeneration Using *n*-Hexane

Criteria	IL14	IL15	IL16	IL17	IL19	IL23
n-Hexane in recycle stream	High <i>n</i> -hexane in recycle stream, additional separation unit to separate the <i>n</i> -hexane from the IL will be required, E-RE using <i>n</i> -hexane is not an ideal regeneration technique using these ILs					High <i>n</i> -hexane in recycle stream, E-RE using <i>n</i> -hexane is not an ideal regeneration technique using these ILs
% IL loss	Negligible IL losses were reported with all shortlisted ILs					
% Loss of <i>n</i> -Hexadecane	High <i>n</i> -hexadecane losses, EDS using these ILs is not an ideal desulfurization technique				High <i>n</i> -hexadecane losses, EDS using these ILs is not an ideal desulfurization technique	
Remaining PPM Sulfur after 6 EDS Stages					High total PPM sulfur was reported after 6 extraction stages, EDS using these ILs is not an ideal desulfurization technique	Satisfactory results if ultra-low sulfur is not the objective

Table 12. Simulation Results from Multiple Extractors in Series (all values in ppm S)

configuration	3 stages	4 stages	6 stages	8 stages
2 extractors in series equal number of stages	248.70	122.36	49.21	33.87
3 extractors in series equal number of stages	45.56	21.88	12.65	11.26
4 extractors in series equal number of stages	11.42	6.53	n/a: ULSD (<10 ppm) has been achieved using four stages	

contrary was observed in this study. Increasing the extraction temperature resulted in a decrease in the desulfurization efficiency using the reported ILs. This could be attributed to the fact that laboratory experiment results might have been tabulated prior to reaching equilibrium, thus reflecting the effect of temperature on mass transfer rather than the extraction efficiency at equilibrium. The Aspen Plus assumes equilibrium is reached and ignores the effects of mass transfer limitations. This should be studied experimentally to provide an estimate of the stage efficiency in the extraction simulation.

The PFD of the optimized EDS and E-RE process using IL17 is shown in Figure 12.

To summarize, for this configuration to work, it is required to use IL17 (1-butyl-3-methylimidazolium thiocyanate) using four EDS columns in series (four stages each), all operated at 25 °C and 1.01325 bar. The loss of *n*-hexadecane increased from 0.02 to 0.06%, which is still very low and can be considered negligible. The E-RE using *n*-hexane is carried out using a three-stage extraction column operated at 25 °C and 1.01325 bar. The E-RE was effective in the removal of DBT from the IL without any loss in the IL, and the removal of thiophene and BT was moderate. It is important to note that using a three-stage extractive regeneration column resulted in the extraction of 42% thiophene, 55% BT, and 90% DBT. This means that E-RE is

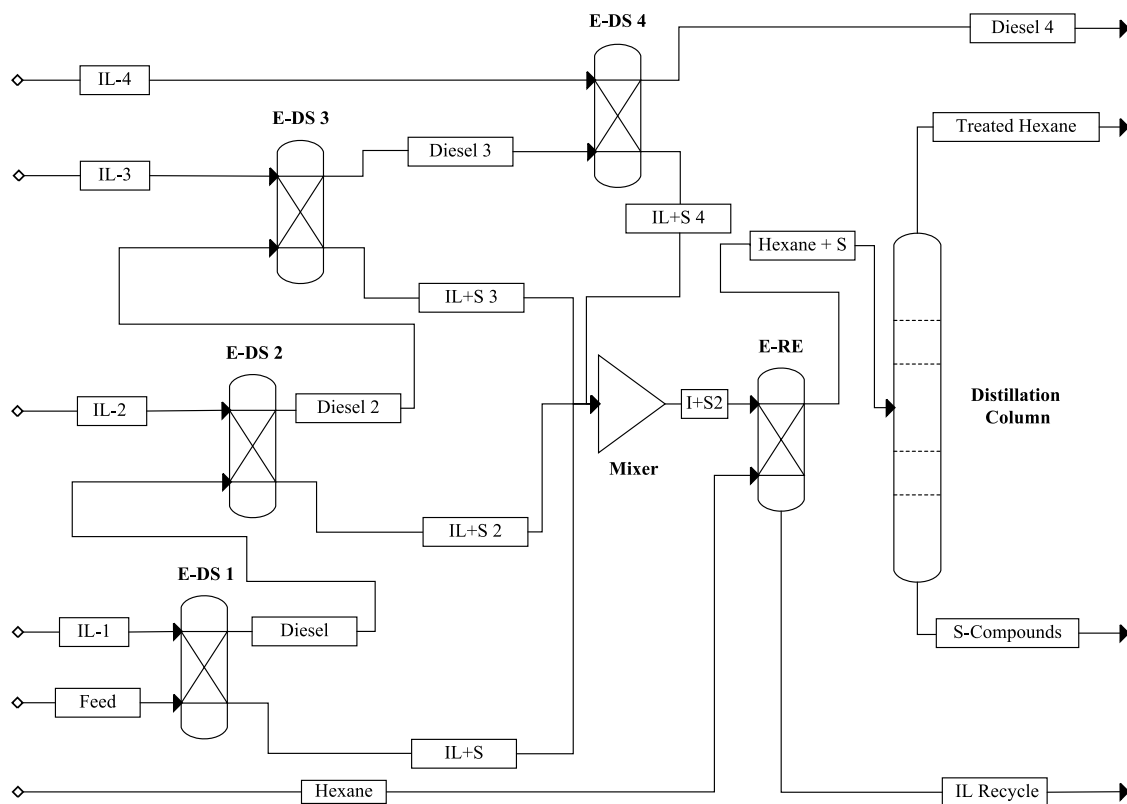


Figure 12. PFD of the optimized EDS and E-RE using IL17.

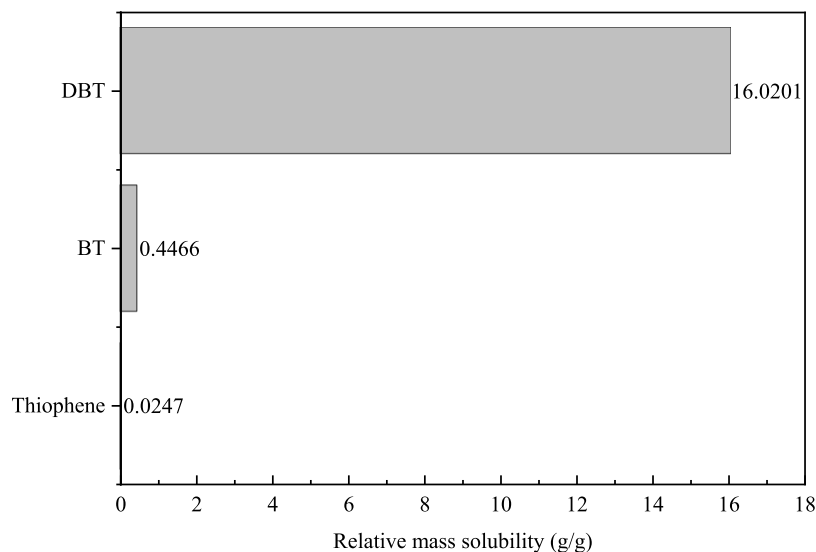


Figure 13. Relative mass solubility of *n*-hexane to thiophene, BT, and DBT.

effective in the removal of DBT from the IL-sulfur stream, but thiophene and BT removal is rather challenging. This can be explained by the relative mass solubility of *n*-hexane to thiophene, BT, and DBT. It can be seen in Figure 13 that DBT is more soluble in *n*-hexane than thiophene and BT; the sulfur compounds (DBT) that are soluble in *n*-hexane are dissolved, leaving the less soluble (thiophene and BT) ones behind. The relative mass solubility is on the order of DBT > BT > thiophene, which is consistent with the removal rates of 90, 55, and 42% DBT, BT, and thiophene, respectively.

Furthermore, since the IL increased by a ratio of 4, the amount of *n*-hexane was increased by the same factor during the regeneration process, and the amount of *n*-hexane in the recycle stream remained unchanged (2.7%). It is true that increased operating costs are attributed to the use of this optimized configuration due to the requirement of an increased amount of IL and *n*-hexane; however, the regeneration of the IL was effective. Additionally, *n*-hexane could be regenerated by stripping away the sulfur components or through distillation, making this process configuration self-sufficient. In this configuration, the sulfur components were removed from *n*-

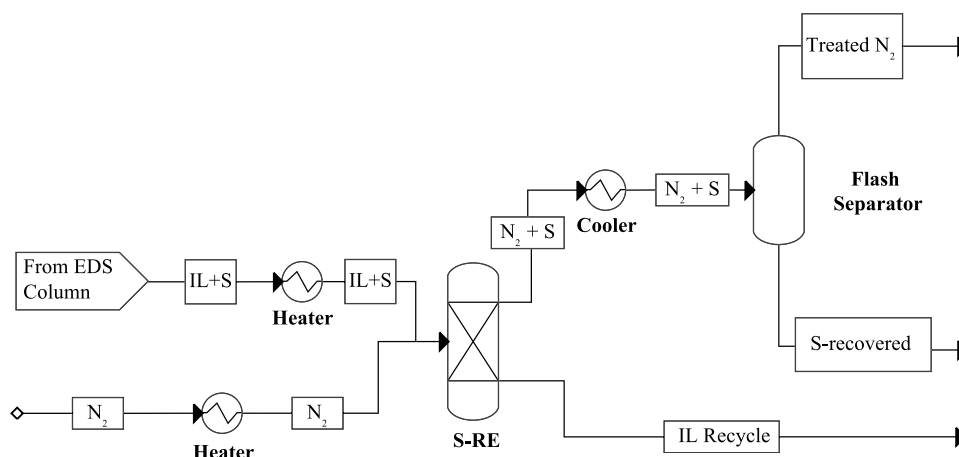


Figure 14. PFD for regeneration using nitrogen as stripping media.

Table 13. Elimination of ILs Based on Criteria for Regeneration by Stripping

IL	Extractive Desulfurization (3 Stages) Total PPM Sulfur	Relative Price (\$/\$)
IL01	365	15.0
IL02	343	11.5
IL03	1,057	52.6
IL04	601	21.7
IL08	1,210	39.8
IL10	1,097	23.9
IL11	869	30.5
IL12	4,334	32.3
IL14	777	22.1
IL15	854	27.0
IL16	1,104	28.7
IL17	1,625	19.4
IL18	1,049	13.7
IL19	1,092	11.9
IL22	2,685	29.6
IL23	744	59.7
IL24	1,001	34.0
IL25	95	46.0
IL26	2,498	22.9
IL05	3,532	18.6
IL06	2,026	36.7
IL07	1,873	101.6
IL09	4,112	19.9
IL13	641	38.9
IL20	2,316	82.2
IL21	2,242	33.1

hexane through a 15-stage distillation column operated at atmospheric conditions. 100% removal of BT and DBT from *n*-hexane was achieved using distillation, but the thiophene amount remained as high as 80% in the treated hexane stream. The reason why hexane/thiophene separation was difficult to achieve via distillation is that hexane-thiophene forms an azeotrope.⁵⁹ This suggests that other separation techniques

need to be explored for the removal of sulfur compounds from *n*-hexane. Furthermore, increased capital costs are required for installation of four EDS columns and one E-RE column as opposed to HDS, which requires fewer separation columns and less capital costs. However, this cost is compensated for by the fact that all of the equipment in this configuration are operated at ambient conditions, which balances out the extra energy costs

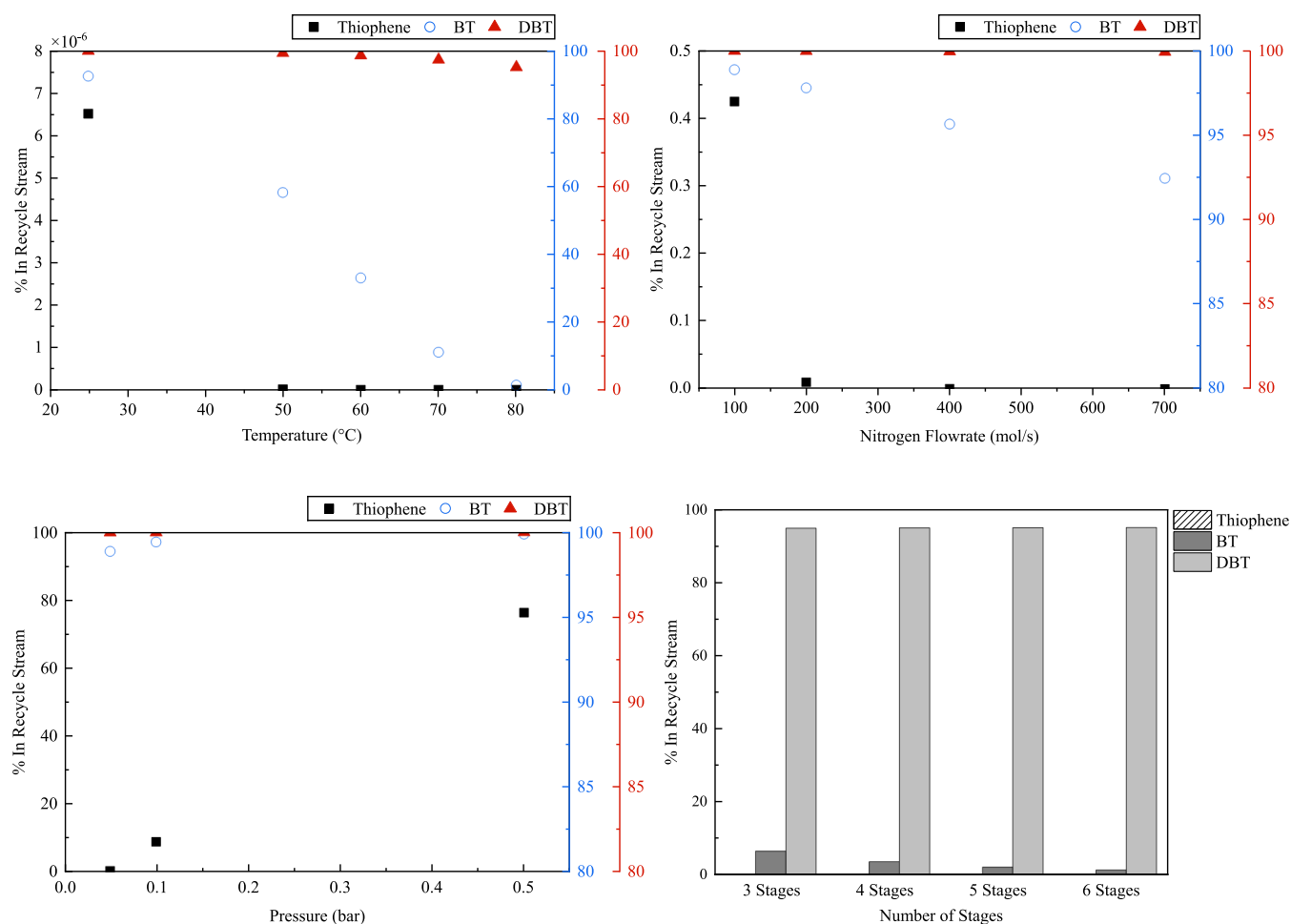


Figure 15. Effect of varying temperature, nitrogen flow rate, pressure, and number of stages on IL regeneration using nitrogen stripping.

required by the harsh operating conditions and excess hydrogen consumption associated with HDS.

6.3. Configuration 2: EDS followed by Regeneration through Nitrogen Stripping or Air Stripping. The regeneration was conceptualized using nitrogen as a stripping medium using IL17 based on the promising results that were obtained from EDS and E-RE. The bottom product of the extractive desulfurization column (EDS) was fed into the regeneration section. The regeneration using nitrogen as stripping media was simulated using the RadFrac column (S-RE) operated without any condenser or reboilers over a range of temperatures, pressures, nitrogen flow rates, and number of stages. In addition, the nitrogen and sulfur components were separated by the use of a condenser (cooler) to condense the sulfur compounds from the gas phase followed by a flash separator operated at 25 °C and 10 bar to separate the condensed sulfur from the nitrogen stream. Figure 14 shows the PFD of the regeneration using nitrogen as the stripping media arrangement.

The same arrangement shown in Figure 14 was followed for air stripping, where the mole fractions were specified as 0.79 N₂ and 0.21 O₂. The effects of varying the column pressure, nitrogen flow rate, temperature, and number of stages were analyzed using IL17 and nitrogen as stripping media. Once these effects were analyzed, the nitrogen flow rate and operating pressure were fixed and the temperature was varied for the rest of the ILs under study. The results were extended to using air as a

stripping medium to study the effectiveness of each stripping medium on the removal of thiophene, BT, and DBT from the spent IL.

6.3.1. IL Regeneration through Stripping Results. A systematic approach was followed to eliminate ILs that are not suited for this process. Certain ILs were eliminated based on their stability, sulfur extraction efficiencies, and system convergence, as listed in Table 13.

As a result, only 9 out of 26 ILs are suited for further study using this configuration. All high-melting-point ILs were eliminated using the above approach and nine low-melting-point ILs remained, namely, IL03, IL10, IL11, IL14, IL15, IL16, IL17, IL19, and IL23. IL17 performance was examined using this configuration by varying the column pressure, nitrogen flow rate, temperature, and number of stages.

6.3.1.1. Varying the Stripping Column Pressure. It is favorable to operate the stripping columns at low pressures. The pressure effects on the removal of thiophene, BT, and DBT from the spent IL stream were analyzed at constant temperature and nitrogen flow rate (25 °C and 100 mol/s N₂) using a six-stage stripping column. It can be seen in Figure 15 that as the stripping column operating pressure is decreased, the amount of thiophene and BT in the IL recycle streams decreased. Pressure effects on DBT were negligible in comparison to thiophene and BT.

6.3.1.2. Varying Nitrogen Flow Rate. The nitrogen flow rate was increased gradually at constant temperature and pressure

Table 14. Percentages of Remaining Sulfur Compounds in the IL Recycle after Nitrogen Stripping

IL	IL03	IL10	IL11	IL14	IL15	IL16	IL17	IL19	IL23
max. temp (°C)	185	200	175	180	140	110	137	120	145
thiophene (%)	0.00	0.00	0.00	0.00	0.00	0.00	0.00	0.00	0.00
BT (%)	0.25	0.00	0.04	0.00	0.46	2.21	0.18	1.03	0.09
DBT (%)	83.27	30.10	75.52	58.90	86.54	91.11	82.80	89.12	80.13

(25 °C, 0.05 bar) as shown in Figure 15. Increasing the nitrogen flow rate into the column reduced the amount of thiophene and BT in the recycle stream and had negligible effects on DBT.

6.3.1.3. Varying the Stripping Column Temperature. The temperatures of the stripping column and feeds were increased gradually at a constant pressure and nitrogen flow rate (0.05 bar, 700 mol/s). The results shown in Figure 15 clearly show that the temperature increase has a significant effect on the removal of BT.

6.3.1.4. Varying the Stripping Column Number of Stages. Increasing the column number of stages at constant temperature, pressure, and nitrogen flow rates (80 °C, 0.05 bar, 700 mol/s) had a positive impact on the removal of thiophene and BT and negligible effects on the removal of DBT. This can be seen in Figure 15. Trace amounts of thiophene were noted at three stages because operating at low pressures and high nitrogen flow rate were sufficient to remove most of the thiophene. The thiophene had been completely removed from the spent IL by moving to a four-stage column.

6.3.1.5. Extension of the Findings to the Remaining ILs. The column number of stages, pressure, and the nitrogen flow rates (six stages, 0.085 bar, 121 mol/s) were fixed for the rest of the ILs, and the temperature was varied until a maximum temperature is reached beyond which further increase in temperature causes the stripping column stages to dry up and the simulation fails to converge. The percentages of remaining sulfur compound in the IL recycle are tabulated in Table 14. It can be seen that the increased difficulty in the removal of DBT is a concern and has been noted with all nine ILs under study.

6.3.2. Process Optimization Results. According to the results, the column operating pressure, nitrogen flow rates, and temperature were all key parameters in the removal of thiophene, BT, and DBT from the spent IL fed to the regeneration column. Decreasing the column operating pressure enhanced the amounts of thiophene and BT in the recycle stream. As the column pressure decreased, the amount of thiophene and BT in recycle streams decreased.

Pressure effects on DBT were negligible in comparison to thiophene and BT. Similarly, increasing the nitrogen flow rate into the column reduced the amount of thiophene and BT in the recycle stream and had a negligible effect on DBT. Reducing the column pressure had a stronger effect on the removal of thiophene, while increasing the nitrogen flow rate had a stronger effect on BT and DBT removal. In addition, increasing the temperature significantly improved the stripping of the heavier sulfur compounds BT and DBT. The effects of changing these parameters can be summarized by referring to Table 15. Hence, it can be concluded that stripping of thiophene could be easily achieved by fixing the pressure and the nitrogen flow rates.

Since temperature was a key variable in determining the stripping efficiencies of BT and DBT, the column number of stages, pressure, and nitrogen flow rates were fixed for the rest of the ILs as tabulated in Table 14. To summarize, IL03, 11, 14, 15, 16, and 19 cannot be coupled with EDS since a significant amount of *n*-hexadecane was lost using this configuration and a

Table 15. Effects of Varying Operating Parameters on the Removal of Thiophene, BT, and DBT from the Spent IL Stream during Regeneration Using Nitrogen Stripping

variable	% increase in the removal of		
	thiophene (%)	BT (%)	DBT (%)
reducing the pressure by half	8.5563	0.5477	0.0055
doubling the nitrogen flow rate	0.4150	1.0728	0.0107
doubling the temperature	0.0000	34.2845	0.6133

large amount of DBT remained in the IL recycle post regeneration. IL10 has the potential to be regenerated using nitrogen stripping since it displayed the lowest amount of DBT in the recycle stream in comparison to other ILs, but it has to be coupled with a desulfurization process other than EDS due to significant loss of *n*-hexadecane. All nine ILs under study resulted in poor removal of DBT. DBT has low volatility and high boiling point (332.5 °C) in comparison to thiophene (84.4 °C) and BT (221 °C); hence, it is difficult to remove using nitrogen stripping. The only two ILs that have the potential to be used under EDS and nitrogen stripping regeneration are IL17 and 23 solely due to the fact that these two ILs have resulted in the lowest losses of *n*-hexadecane. IL17 and 23 both had a large amount of DBT post nitrogen stripping; therefore, it is suggested that their regeneration should be coupled with extractive regeneration. Extractive regeneration could be performed prior to nitrogen stripping to remove most of the thiophene, BT, and DBT, and their traces could be removed by a subsequent nitrogen stripping column. Recalling that IL23 cannot be used in E-RE due to the high amount of *n*-hexane present in the recycle stream, it can be concluded that IL17, namely, 1-butyl-3-methylimidazolium thiocyanate, is the most promising IL for all configurations that were under study. A summary of these findings can be seen in Table 16.

IL17 was further optimized, and the lowest pressure that the column could be operated was found to be 0.08 bar, the maximum temperature was 137 °C, and the maximum nitrogen flow rate was 121 mol/s through which 100% thiophene, 100% BT, and 18.7% DBT were stripped. Negligible differences were noted using air as a stripping medium. 100% thiophene, 100% BT, and 18.16% DBT were stripped using the same optimized conditions as nitrogen stripping.

It can be deduced that air stripping and nitrogen stripping both have the same results, and either of them could be used as a regeneration approach. It can be seen that DBT is the hardest component to strip in comparison to thiophene and BT. The method used for the separation of nitrogen and sulfur components (condensation followed by flash separation) resulted in the removal of 84% thiophene, 99.95% BT, and 100% DBT from the nitrogen/air stream. The U.S. EPA standards limit the sulfur emissions from waste gas to less than 2500 ppmv;⁶⁰ the proposed sulfur recovery method results in 595 ppmv in the waste gas stream. Therefore, separation using this technique was efficient and no further treatment is required. Furthermore, since the removal of DBT using nitrogen or air

Table 16. Discussion of the Nine Shortlisted ILs for Regeneration Using Nitrogen Stripping

IL03	IL10	IL11	IL14	IL15	IL16	IL17	IL19	IL23
EDS results using single extraction column were satisfactory					EDS results using single extraction column were not satisfactory			
Significant amount of n-hexadecane was lost during EDS						Negligible amount of n-hexadecane was lost during EDS	Significant amount of n-hexadecane was lost during EDS	Negligible amount of n-hexadecane was lost during EDS
100% of thiophene and 99.7% BT were removed from spent IL stream	100% of thiophene and BT were removed from spent IL stream		100% of thiophene and 99.5% BT were removed from spent IL stream	100% of thiophene and 97.8% BT were removed from spent IL stream	100% of thiophene and 99.8% BT were removed from spent IL stream	100% of thiophene and 99% BT were removed from spent IL stream	100% of thiophene and 99.9% BT were removed from spent IL stream	100% of thiophene and 99.9% BT were removed from spent IL stream
DBT was not efficiently removed using Nitrogen stripping	DBT was sufficiently removed using Nitrogen stripping in comparison to other ILs	DBT was not efficiently removed using Nitrogen stripping						

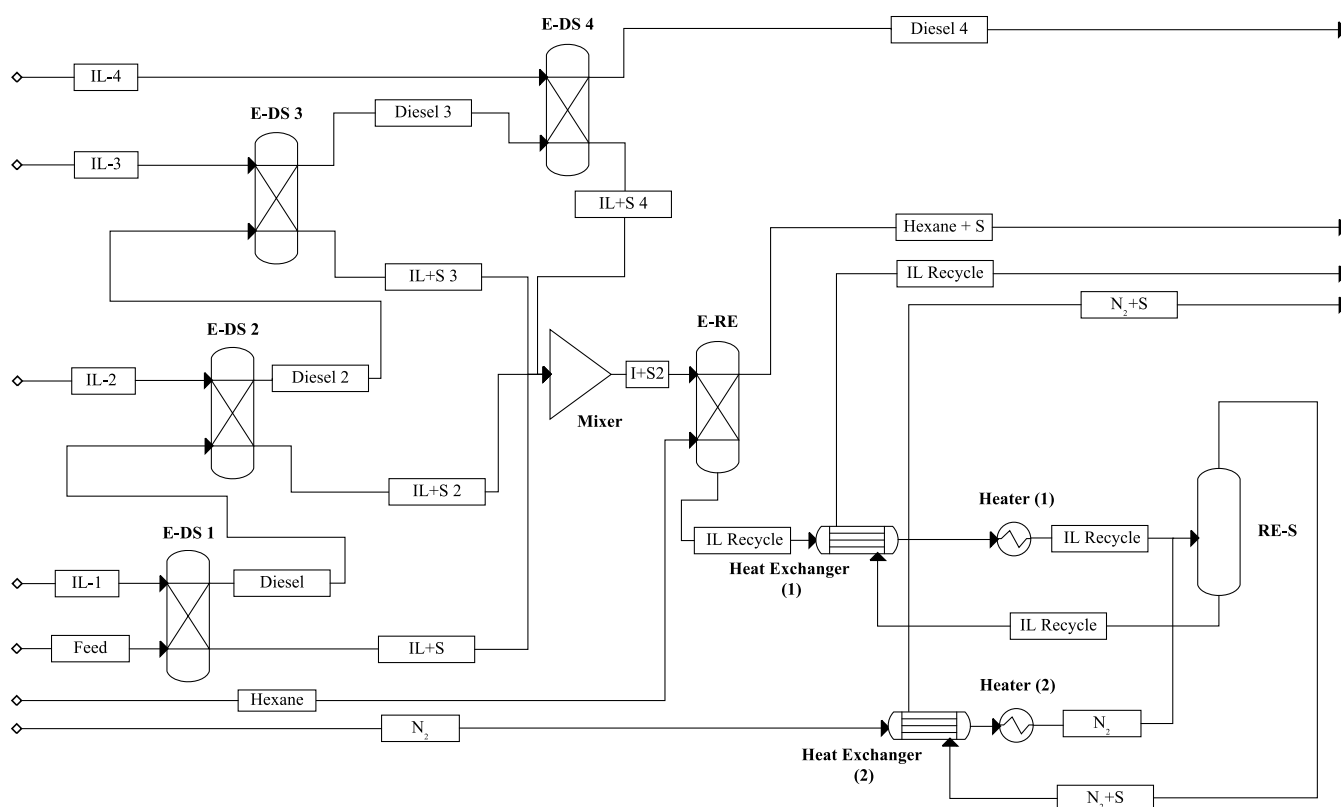


Figure 16. PFD for the proposed overall desulfurization and regeneration process using IL17.

stripping was not efficient, regeneration using nitrogen or air stripping may not be the ideal process for the regeneration of ILs post extractive desulfurization. Better results may be obtained

when coupled with oxidative desulfurization since the dibenzothiophenes are released as dibenzothiophene oxides (sulfones), which are easier to strip. Another suggested method

Table 17. Key Stream Flow Rates for the Proposed Overall Desulfurization and Regeneration Process Using IL17 (all values in kg/h)

stream	<i>n</i> -hexadecane	thiophene	BT	DBT	IL17	<i>n</i> -hexane	N ₂	total mass flow
model diesel feed	75,579	347	2,908	83	0	0	0	78,916
IL feed	0	0	0	0	284,121	0	0	284,121
treated diesel	75,527	0	0	3	0	0	0	75,530
I + S (IL + sulfur compounds)	51	347	2,908	80	284,121	0	0	287,507
<i>n</i> -hexane	0	0	0	0	0	124,095	0	124,095
<i>n</i> -hexane + extracted sulfur	51	145	1,608	72	0	120,688	0	122,564
N ₂	0	0	0	0	0	0	12,203	12,203
N ₂ + stripped sulfur	0	201	921	1	0	3,407	12,201	16,731
IL recycle stream	0	0	379	8	284,121	0	2	284,509

Table 18. Energy Analysis Results from Aspen Plus Simulation

heat exchanger	heat exchanger details					
	base duty (MJ/h)	hot inlet temperature (°C)	hot outlet temperature (°C)	cold inlet temperature (°C)	cold outlet temperature (°C)	base area (m ²)
heat exchanger (1)	48,669	136	40	25	120	2,853
heat exchanger (2)	1,193	136	80	25	119	4,090
heater (1)	9,426	175	174	120	137	82
heater (2)	231	175	174	119	137	197
utilities	energy (MJ/h)					
MP steam	9,657					
total utilities	9,657					

is to couple it with E-RE to remove most of the DBT prior to S-RE.

6.4. Configuration 3: Combination of EDS, E-RE, and S-RE. The results suggest that operating several extractive desulfurization columns in series along with combined extractive regeneration and regeneration through stripping would result in high desulfurization efficiency, minimal losses of *n*-hexadecane and ILs, as well as negligible amounts of contaminants (*n*-hexane, thiophene, BT, and DBT) in the IL recycle stream. Recalling the following:

- Four, 4-stage extractive desulfurization columns operated in series at ambient conditions (25 °C, 1.01325 bar) resulted in 6.53 ppm total sulfur.
- A three-stage extractive regeneration column using *n*-hexane at ambient conditions (25 °C, 1.01325 bar) resulted in the removal of 42% thiophene, 55% BT, and 90% DBT from the IL recycle stream.
- A three-stage regeneration column through nitrogen stripping removed 100% thiophene, 97% BT, and 17% DBT at 0.085 bar and 137 °C.

It can be concluded that extractive regeneration could compensate for the low DBT removal associated with the use of nitrogen in S-RE. Similarly, S-RE using nitrogen as a stripping medium could compensate for the fairly low thiophene and BT removal from the IL recycle stream. This suggests that if an overall process is designed using the above findings, a solution to all of the discussed concerns could be proposed. The overall process was simulated using IL17 in Aspen Plus as per the PFD shown in Figure 16.

The suggested process can achieve ULSD with only 6.53 ppm total sulfur from a 10,500 ppm total sulfur feed. The combined regeneration technique resulted in 100% IL being recycled containing 0% thiophene, 10% BT, and 12% DBT of the original amounts. The total flow rates and operating conditions of the key streams can be found in Table 17. When considering the

overall process involving the utilization of four EDS columns, the ratio of ionic liquid (IL) to feed is estimated to be approximately 3.595 on a mass basis.

6.5. Energy Analysis. As mentioned earlier, one of the motivations for using extractive desulfurization is to reduce energy consumption relative to the traditional HDS process. While most of the optimized processes shown in Figure 16 are conducted under ambient conditions, the nitrogen stripping section requires the use of steam heating to raise the temperatures of the inlet gas and liquid from ambient temperature to 137 °C. With heat integration involving the use of hot exit streams to preheat the inlet streams, the steam requirements are significantly reduced. The results of energy analysis from Aspen Plus are shown in Table 18. For comparison, the energy requirements in the traditional hydrodesulfurization process, as reported in a recent literature study,⁶¹ are also shown in Table 19. To enable a fair comparison, the energy required per kg of sulfur removed has also been calculated for each process. It is observed that the optimized IL desulfurization process has a requirement of 2.896 MJ/kg sulfur removed, which is significantly lower than that of the hydrodesulfurization process, 8.219 MJ/kg sulfur removed. Therefore, when compared based on energy consumption, the proposed process shows a significant advantage over the traditional desulfurization process.

7. DISCUSSION OF RESULTS

The EDS configuration was studied for 26 commercially available ILs and complemented with two regeneration methods: extractive regeneration using *n*-hexane and regeneration through nitrogen and/or air stripping. IL screening criteria resulted in six possible ILs for extractive regeneration and nine ILs for regeneration using nitrogen or air stripping. For the six ILs under study in extractive regeneration, the number of extractive desulfurization stages was varied and their effect on the desulfurization efficiency and the amount of *n*-hexadecane

Table 19. Comparison of Energy Requirements between Conventional Hydrodesulfurization Process and Proposed Desulfurization and Regeneration Process Using IL17

stream	literature results (conventional hydrodesulfurization process)		proposed desulfurization and regeneration process using IL17	
	total amount of sulfur (kg/h)		total amount of sulfur (kg/h)	
feed				
feed 1	4,220		347	thiophene in feed
feed 2	286		2,908	BT in feed
feed 3	1,477		82.9	DBT in feed
product	13.35		0.004	thiophene in product
			0.205	BT in product
			2.544	DBT in product
total amount of sulfur in the feed (kg/h)	5,983		3,338	
total amount of sulfur in the product (kg/h)	13.348		2.753	
amount of sulfur removed	5,969		3,335	
total energy requirements (MJ/h)	49,064		9,657	
energy requirement per mass sulfur removed (MJ/kg S)	8.219		2.896	

lost were examined. The amount of IL and extractant (*n*-hexane) in the recycle stream were also studied. These criteria enabled the determination of the most promising IL for this configuration, namely, IL17 (1-butyl-3-methylimidazolium thiocyanate). This IL has shown the lowest amount of *n*-hexadecane loss in comparison to other ILs under study post extractive desulfurization. It is desired to maintain minimum losses of *n*-hexadecane as it represents the main product (diesel). The high losses of *n*-hexadecane observed in our Aspen Plus simulation of EDS using other ILs can be attributed to the properties of the ILs used and the assumptions made in the simulation model. Further studies are needed to optimize the process conditions and IL properties to minimize the loss of *n*-hexadecane and improve the efficiency of the EDS process for the ILs that depicted this behavior. Furthermore, the amount of *n*-hexane present in the recycle stream post E-RE of IL17 was relatively low and zero losses of IL were observed.

Despite being the best option, IL17 still showed high total PPM sulfur in the treated diesel stream; this suggests that the proposed regeneration techniques work well with the said IL, but consideration should be given to using other desulfurization techniques or to optimizing the EDS section. This could be achieved through increasing the number of stages of the EDS column, carrying out several EDS in series, or through coupling it with a different desulfurization method to achieve the desired level of desulfurization. In addition, E-RE using the proposed method was efficient in the removal of DBT and fair in the removal of thiophene and BT from the spent IL stream. This demonstrates that E-RE using *n*-hexane is a good technique in the removal of stubborn DBT.

On the other hand, regeneration using nitrogen as a stripping medium resulted in complete removal of thiophene and BT, but the removal of DBT from the spent IL stream was found to be challenging for all nine ILs under study using this configuration. In the regeneration using nitrogen as a stripping medium, IL17

was again suggested as the most promising IL. The effects of pressure, temperature, nitrogen flow rate, and stripping column number of stages were analyzed. It was found that thiophene and BT were easily stripped from the spent IL stream at pressures below 1 bar and nitrogen flow rates of no more than 100 mol/s. The removal of DBT was the most challenging, and it was found that temperature was the key parameter that determines the removal of high- M_w sulfur compounds (BT and DBT). S-RE would generate better results when coupled with oxidative desulfurization since the dibenzothiophenes are released as dibenzothiophene oxides (sulfones), which are easier to strip. Another suggested method is to couple it with E-RE to remove most of the DBT prior to S-RE. In addition, no improvement in the regeneration was noted when air was used as a stripping media and the results were very similar to those obtained using nitrogen.

Furthermore, the separation of the sulfur components from the extractant/stripping media should be taken into consideration. The separation of the sulfur components in E-RE was carried out using a distillation column operated at atmospheric conditions (25 °C and 1.01325 bar). This separation method resulted in complete removal of BT and DBT. However, the method resulted in 80% thiophene being entrained within the *n*-hexane stream. This suggests that other techniques should be explored for the separation of *n*-hexane from sulfur. In S-RE, the separation of sulfur components from nitrogen/air was achieved through condensation and flash separation at 25 °C and 10 bar. The method resulted in the complete removal of BT and DBT, and only 16% thiophene remained in the nitrogen/air stream.

In summary, the results indicate that IL17 is the most promising IL among all 26 ILs under study in terms of EDS, E-RE, and S-RE. As a result, an optimized diesel desulfurization process that is a combination of all configurations under study has been proposed. This was necessary to obtain ULSD and complete removal of thiophene, BT, and DBT from the spent IL stream without imposing contaminants such *n*-hexane and with minimum losses of *n*-hexadecane. The proposed process was able to achieve ULSD with 6.53 PPM total sulfur, 0.06% loss of *n*-hexadecane, and 100% of the IL being recycled, and the recycled stream contained 0% thiophene, 10% BT, and 12% DBT of the original amounts. There are several sources that contribute to errors in the simulation results, and minimizing the effect of the errors is crucial for future works that intend to use the methods highlighted within this work. The possible sources of error in simulation results include the following:

- Parameters such as normal boiling points, critical properties, CPIG, and CPLDIP necessary for the database creation and use of the COSMO-SAC property model in Aspen Plus were calculated using group contribution methods and models. The simulations were carried out under the assumption that these methods and models are accurate, while in reality, all models have a certain degree of error associated with their use.
- The viscosity of the ILs under study was not taken into consideration. Viscosities are important in determining the stage efficiencies of the columns. All simulations were carried out assuming 100% stage efficiencies, and ultimately, pilot plant studies are required where a higher number of stages will be required based on carefully predicted stage efficiencies.
- With regard to the results obtained with S-RE, it was noted that DBT removal is rather challenging in part due

to its low volatility and high boiling point. According to the simulation results, some of the DBT was removed; this is mainly due to the fact that Aspen Plus simulations did not take into consideration the kinetics. The simulations were conducted solely based on thermodynamic relationships, and that is why, eventually some of the DBT was removed.

8. CONCLUSIONS

In this work, quantum and statistical thermodynamic calculations and property estimation methods were utilized to incorporate ionic liquids (ILs) into Aspen Plus for the simulation of desulfurization processes to enable IL screening, process design, and IL regeneration analysis. A database of 26 commercially available ILs was generated that contains all necessary properties for simulating IL processes in Aspen Plus using the COSMO-SAC property package without the need for extensive experimental work. The key findings from this study demonstrate that E-RE, using *n*-hexane as the regeneration solvent, is a promising and efficient method for removing dibenzothiophene (DBT) and shows reasonable efficiency in the removal of thiophene and benzothiophene (BT) from spent IL. Alternatively, S-RE can be used for the complete removal of thiophene and BT but not for the removal of DBT from the spent IL. Furthermore, temperature was found to be the key controlling factor affecting the removal of high- M_w sulfur compounds such as BT and DBT. In addition, the performance of the S-RE method was not affected when air was used as a stripping medium instead of pure nitrogen, and the results were almost identical.

Combining the traditional EDS with both regeneration methods could be a very promising technique to achieve ultralow sulfur diesel (ULSD). The proposed combined process achieved ULSD with 6.53 ppm total sulfur, 0.06% loss of *n*-hexadecane, and 100% IL recycling, and the recycled stream contained 0% thiophene, 10% BT, and 12% DBT of the original amounts. The approach used to evaluate the desulfurization of several ILs in this study can be extended to simulate alternative desulfurization processes such as oxidative desulfurization (ODS).

In this study, the extractive regeneration of ILs was examined using *n*-hexane, but the performance of extractants other than *n*-hexane, such as pentane and cyclohexane, could also be studied. Additionally, it is important to note that the viscosity of the ILs studied was not taken into consideration, which is important in determining the stage efficiencies of the columns. All simulations were carried out assuming 100% stage efficiencies, and pilot plant studies should be conducted to determine the required number of stages based on estimated stage efficiencies.

Finally, a detailed economic study is necessary to fully validate the potential of industrializing the proposed process or any of the configurations discussed. The qualitative economic analysis depicted in Table 20 suggests that the proposed process has potential advantages in terms of desulfurization efficiency and environmental impact. The process provides a technically feasible and environmentally benign alternative to hydrodesulfurization, but the challenge lies in the trade-off of capital and operating costs. The loss of IL is the most critical economic consideration for IL-assisted processes due to the current high cost of most ILs. However, the success of complete IL regeneration achieved by the proposed process indicates that this approach may hold potential. With increasing attention on

Table 20. Qualitative Economic and Environmental Analyses of Alternative Process Configurations for Diesel Desulfurization

criteria	HDS	EDS followed by E-RE	EDS followed by S-RE	combined process
desulfurization efficiency	inefficient in the removal of BT and DBT	effective in the removal of high- M_w sulfur compounds such as BT and DBT	effective in the removal of high- M_w sulfur compounds such as BT and DBT	effective in the removal of high- M_w sulfur compounds such as BT and DBT
capital cost		high—additional extraction units are required to achieve ULSD	high—additional extraction units are required to achieve ULSD	high—additional extraction units are required to achieve ULSD
operating cost	energy-intensive; harsh operating conditions are required; high consumption of H_2 , which is not efficiently recycled	low energy costs; ambient operating conditions are required for all equipment; ILs are effectively regenerated and recycled	medium energy requirements: ambient operating conditions are required for extraction columns, low pressures and high temperatures are required for the stripping column, ILs are effectively regenerated and recycled	medium energy requirements: ambient operating conditions are required for extraction columns, low pressures and high temperatures are required for the stripping column, ILs are effectively regenerated and recycled
environmental considerations	high hydrogen consumption and energy-intensive	low environmental impact; IL fully recycled	low environmental impact; IL fully recycled	low environmental impact; IL fully recycled

ILs for industrial use, it is expected that increasing demand will enable scaled-up production and reduce their price on the bulk scale. At that stage, a detailed economic analysis can be conducted to validate the assumptions and provide a deeper insight into the feasibility of the proposed configurations versus the existing HDS process.

■ ASSOCIATED CONTENT

SI Supporting Information

The Supporting Information is available free of charge at <https://pubs.acs.org/doi/10.1021/acsomega.3c01952>.

Assessment of the extraction efficiencies of 26 commercially available ILs using COSMOtherm, a software package that uses quantum chemical calculations to predict the thermodynamic properties of molecules; Aspen Plus software was used to set up and validate the results obtained from the COSMOtherm calculations, with two different implementations of the COSMO-based thermodynamic approach (COSMO-RS and COSMO-SAC) available for use, and a summary of the various factors and conditions studied via simulation (PDF)

Database containing the calculated parameters and properties of the ionic liquids under study (XLSX)

■ AUTHOR INFORMATION

Corresponding Author

Paul Nancarrow – Department of Chemical & Biological Engineering, American University of Sharjah, Sharjah P.O. Box 26666, United Arab Emirates; orcid.org/0000-0002-6188-8491; Phone: +971 6 515 4903; Email: pnancarrow@aus.edu

Authors

Haifa Ben Salah – Department of Chemical & Biological Engineering, American University of Sharjah, Sharjah P.O. Box 26666, United Arab Emirates

Amani Al Othman – Department of Chemical & Biological Engineering, American University of Sharjah, Sharjah P.O. Box 26666, United Arab Emirates

Complete contact information is available at: <https://pubs.acs.org/doi/10.1021/acsomega.3c01952>

Notes

The authors declare no competing financial interest.

■ ACKNOWLEDGMENTS

The work in this paper was supported, in part, by the Open Access Program from the American University of Sharjah. This paper represents the opinions of the authors and does not mean to represent the position or opinions of the American University of Sharjah.

■ REFERENCES

- (1) Domingo, J. L.; Rovira, J. Effects of air pollutants on the transmission and severity of respiratory viral infections. *Environ. Res.* **2020**, *187*, No. 109650.
- (2) Burns, D. A.; Aherne, J.; Gay, D. A.; Lehmann, C.M.B. Acid rain and its environmental effects: Recent scientific advances. *Atmos. Environ.* **2016**, *146*, 1–4.
- (3) US: Fuels: Diesel and Gasoline | Transport Policy, (n.d.), 2020. <https://www.transportpolicy.net/standard/us-fuels-diesel-and-gasoline/> (accessed April 17, 2020).
- (4) Verheugen, G. Case No COMP/M.5445 - REGULATION (EC) No 139/2004, n.d., 2020. https://ec.europa.eu/search/?queryText=diesel+sulfur+content+&query_source=europa_default&filterSource=europa_default&swlang=en&more_options_language=en&more_options_f_formats=&more_options_date= (accessed April 17, 2020).
- (5) Parkash, S. Distillate Hydrotreating. In *Refining Processes Handbook*; Gulf Professional Publishing, 2003; pp 29–61.
- (6) Houda, S.; Lancelot, C.; Blanchard, P.; Poinel, L.; Lamonier, C. Oxidative Desulfurization of Heavy Oils with High Sulfur Content: A Review. *Catalysts* **2018**, *8*, No. 34.
- (7) Subhan, F.; Aslam, S.; Yan, Z.; Yaseen, M. Highly dispersive Cu species constructed in mesoporous silica derived from ZSM-5 for batch and continuous adsorptive desulfurization of thiophene. *Fuel Process. Technol.* **2022**, *235*, No. 107351.
- (8) Speight, J. G.; El-Gendy, N. S. Biocatalytic Desulfurization. In *Introduction to Petroleum Biotechnology*; Gulf Professional Publishing, 2018; pp 165–227.
- (9) Robinson, P. R.; Dolbear, G. E. Hydrotreating and Hydrocracking: Fundamentals. In *Practical Advances in Petroleum Processing*; Hsu, C. S.; Robinson, P. R., Eds.; Springer, 2006; pp 177–218.
- (10) Shafi, R.; Hutchings, G. J. Hydrodesulfurization of hindered dibenzothiophenes: an overview. *Catal. Today* **2000**, *59*, 423–442.
- (11) Welton, T. Ionic liquids in catalysis. *Coord. Chem. Rev.* **2009**, *248*, 2459–2477.
- (12) Xu, R.; Pang, W.; Huo, Q. *Modern Inorganic Synthetic Chemistry*; Elsevier, 2011.
- (13) Salah, H. B.; Nancarrow, P.; Al-Othman, A. Ionic liquid-assisted refinery processes – A review and industrial perspective. *Fuel* **2021**, *302*, No. 121195.
- (14) Hanson, C.; Patel, A. N.; Chang-Kakoti, D. K. Separation of thiophene from benzene by solvent extraction. *I. J. Appl. Chem.* **2007**, *19*, 320–323.
- (15) Zhang, W.; Hou, K.; Mi, G.; Chen, N. Liquid-liquid equilibria of the ternary system thiophene + octane + dimethyl sulfoxide at several temperatures. *Appl. Biochem. Biotechnol.* **2010**, *160*, 516–522.
- (16) Tao, B.; Li, X.; Yan, M.; Luo, W. Solubility of dibenzothiophene in nine organic solvents: Experimental measurement and thermodynamic modelling. *J. Chem. Thermodyn.* **2019**, *129*, 73–82.
- (17) Saha, B.; Sengupta, S.; Selvin, R. Comparative studies of extraction ability of organic solvents to extract thiophene from model fuel. *Sep. Sci. Technol.* **2020**, *55*, 1123–1132.
- (18) Shekaari, H.; Zafarani-Moattar, M. T.; Mohammadi, B. Liquid-liquid equilibria and thermophysical properties of ternary mixtures {(benzene / thiophene) + hexane + deep eutectic solvents}. *Fluid Phase Equilib.* **2020**, *509*, No. 112455.
- (19) Lima, F.; Branco, L. C.; Silvestre, A.J.D.; Marrucho, I. M. Deep desulfurization of fuels: Are deep eutectic solvents the alternative for ionic liquids? *Fuel* **2021**, *293*, No. 120297.
- (20) Abro, R.; Kiran, N.; Ahmed, S.; Muhammad, A.; Jatoti, A. S.; Mazari, S. A.; Salma, U.; Plechkova, N. V. Extractive desulfurization of fuel oils using deep eutectic solvents – A comprehensive review. *J. Environ. Chem. Eng.* **2022**, *10*, No. 107369.
- (21) Abdullah, S.; Aziz, H.; Man, Z. Ionic Liquids for Desulphurization: A Review. In *Recent Advances in Ionic Liquids*; IntechOpen, 2018.
- (22) Butt, H. S.; Lethesh, K. C.; Fiksdahl, A. Fuel oil desulfurization with dual functionalized imidazolium based ionic liquids. *Sep. Purif. Technol.* **2020**, *248*, No. 116959.
- (23) Ahmed, O. U.; Mjalli, F. S.; Talal, A.-W.; Al-Wahaibi, Y.; Al Nashef, I. M. Extractive Desulfurization of Liquid Fuel using Modified Pyrrolidinium and Phosphonium Based Ionic Liquid Solvents. *J. Solution Chem.* **2018**, *47*, 468–483.
- (24) Yan, J.; Luo, F.; Du, Y.; Yi, Q.; Hao, X.; Dong, H.; Sun, L. Extraction desulfurization with mixed solvents of organic solvent + organic solvent or deep eutectic solvent as extractants: Liquid-liquid equilibrium experiments and molecular dynamics simulations. *Fluid Phase Equilib.* **2023**, *565*, No. 113655.
- (25) Dharaskar, S. A.; Wasewar, K.; Varma, M.; Shende, D. Ionic Liquids: Environmentally Benign Solvent for Extractive Deep-

- desulfurization of Liquid Fuels. *J. Mod. Chem. Chem. Technol.* **2014**, *5*, 28–34.
- (26) Andevary, H. H.; Akbari, A.; Omidkhan, M. High efficient and selective oxidative desulfurization of diesel fuel using dual-function [Omicron]FeCl₄ as catalyst/extractant. *Fuel Process. Technol.* **2019**, *185*, 8–17.
- (27) Jiang, B.; Yang, H.; Zhang, L.; Zhang, R.; Sun, Y.; Huang, Y. Efficient oxidative desulfurization of diesel fuel using amide-based ionic liquids. *Chem. Eng. J.* **2016**, *283*, 89–96.
- (28) Zolotareva, D.; Zazybin, A.; Rafikova, K.; Dembitsky, V. M.; Dauletbakov, A.; Yu, V. Ionic liquids assisted desulfurization and denitrogenation of fuels. *Vietnam J. Chem.* **2019**, *57*, 133–163.
- (29) Li, X.; Zhang, J.; Zhou, F.; Wang, Y.; Yuan, X.; Wang, H. Oxidative desulfurization of dibenzothiophene and diesel by hydrogen peroxide: Catalysis of H₃PMo₁₂O₄₀ immobilized on the ionic liquid modified SiO₂. *Mol. Catal.* **2018**, *452*, 93–99.
- (30) Zhang, M.; Wang, M.; Yang, J.; Li, H.; Liu, J.; Chen, X.; Zhu, W.; Li, H. Polyoxometalate-based silica-supported ionic liquids for heterogeneous oxidative desulfurization in fuels. *Pet. Sci.* **2018**, *15*, 882–889.
- (31) Chen, X.; Zhang, M.; Wei, Y.; Li, H.; Liu, J.; Zhang, Q.; Zhu, W.; Li, H. Ionic liquid-supported 3DOM silica for efficient heterogeneous oxidative desulfurization. *Inorg. Chem. Front.* **2018**, *5*, 2478–2485.
- (32) Du, Y.; Zhou, L.; Guo, Z.; Du, X.; Lei, J. Preparation of ordered meso/macroporous HPW/titania–silica catalyst for efficient oxidative desulfurization of model fuel. *J. Porous Mater.* **2019**, *26*, 1069–1077.
- (33) Ahmad, M.; Aslam, S.; Subhan, F.; Zhen, L.; Yan, Z.; Yaseen, M.; Ikram, M.; Nazir, A. Sn-doped nanoconfinements of SBA-15 for oxidative desulfurization: Kinetics and thermodynamics. *Fuel* **2023**, *346*, No. 128372.
- (34) Dharaskar, S. A.; Wasewar, K. L.; Varma, M. N.; Shende, D. Z. Synthesis, characterization, and application of 1-butyl-3-methylimidazolium thiocyanate for extractive desulfurization of liquid fuel. *Environ. Sci. Pollut. Res.* **2016**, *23*, 9284–9294.
- (35) Wang, Q.; Zhang, T.; Zhang, S.; Fan, Y.; Chen, B. Extractive desulfurization of fuels using trialkylamine-based protic ionic liquids. *Sep. Purif. Technol.* **2020**, *231*, No. 115923.
- (36) Zhang, S.; Zhang, Q.; Zhang, Z. C. Extractive Desulfurization and Denitrogenation of Fuels Using Ionic Liquids. *Ind. Eng. Chem. Res.* **2004**, *43*, 614–622.
- (37) Kiran, N.; Abro, R.; Abro, M.; Shah, A. A.; Jatoi, A. S.; Bhutto, A. W.; Qureshi, K.; Sabzoi, N.; Gao, S.; Yu, G. Extractive desulfurization of gasoline using binary solvent of Bronsted-based ionic liquids and non-volatile organic compound. *Chem. Pap.* **2019**, *73*, 2757–2765.
- (38) Mochizuki, Y.; Sugawara, K. Removal of Organic Sulfur from Hydrocarbon Resources Using Ionic Liquids. *Energy Fuels* **2008**, *22*, 3303–3307.
- (39) Fonseca, R. S. P.; Silva, F. C.; Sinfrônio, F. S. M.; de J S Mendonça, C.; dos S Neto, I. S. Synthesis of Morpholine-Based Ionic Liquids for Extractive Desulfurization of Diesel Fuel. *Braz. J. Chem. Eng.* **2019**, *36*, 1019–1027.
- (40) Renon, H.; Prausnitz, J. M. Local compositions in thermodynamic excess functions for liquid mixtures. *AIChE J.* **1968**, *14*, 135–144.
- (41) Maurer, G.; Prausnitz, J. M. On the derivation and extension of the uniquac equation. *Fluid Phase Equilib.* **1978**, *2*, 91–99.
- (42) Fredenslund, A.; Jones, R. L.; Prausnitz, J. M. Group-contribution estimation of activity coefficients in nonideal liquid mixtures. *AIChE J.* **1975**, *21*, 1086–1099.
- (43) Klamt, A. Conductor-like Screening Model for Real Solvents: A New Approach to the Quantitative Calculation of Solvation Phenomena. *J. Phys. Chem. A* **1995**, *99*, 2224–2235.
- (44) Lin, S.-T.; Sandler, S. I. A Priori Phase Equilibrium Prediction from a Segment Contribution Solvation Model. *Ind. Eng. Chem. Res.* **2002**, *41*, 899–913.
- (45) Mahmoudabadi, S. Z.; Pazuki, G. Investigation of COSMO-SAC model for solubility and cocrystal formation of pharmaceutical compounds. *Sci. Rep.* **2020**, *10*, No. 19879.
- (46) TURBOMOLE Program Package for Electronic Structure Calculations. TURBOMOLE. (n.d.), 2020. <https://www.turbomole.org/> (accessed July 20, 2020).
- (47) BIOVIA Solvation Chemistry - BIOVIA - Dassault Systèmes, (n.d.), 2020. <https://www.3ds.com/products-services/biovia/products/molecular-modeling-simulation/solvation-chemistry/> (accessed July 20, 2020).
- (48) Ferro, V. R.; Moya, C.; Moreno, D.; Santiago, R.; de Riva, J.; Pedrosa, G.; Larriba, M.; Diaz, I.; Palomar, J. Enterprise Ionic Liquids Database (ILUAM) for Use in Aspen ONE Programs Suite with COSMO-Based Property Methods. *Ind. Eng. Chem. Res.* **2018**, *57*, 980–989.
- (49) Nancarrow, P.; Mustafa, N.; Shahid, A.; Varughese, V.; Zaffar, U.; Ahmed, R.; Akther, N.; Ahmed, H.; AlZubaidy, I.; Hasan, S.; Elsayed, Y.; Sara, Z. Technical Evaluation of Ionic Liquid-Extractive Processing of Ultra Low Sulfur Diesel Fuel. *Ind. Eng. Chem. Res.* **2015**, *54*, 10843–10853.
- (50) ADNOC Crude Oil Product Specifications, (n.d.), 2021. <https://adnoc.ae/en/our-products/product-specification> (accessed January 28, 2021).
- (51) Valderrama, J. O.; Robles, P. A. Critical Properties, Normal Boiling Temperatures, and Acentric Factors of Fifty Ionic Liquids. *Ind. Eng. Chem. Res.* **2007**, *46*, 1338–1344.
- (52) Ge, R.; Hardacre, C.; Jacquemin, J.; Nancarrow, P.; Rooney, D. W. Heat Capacities of Ionic Liquids as a Function of Temperature at 0.1 MPa. Measurement and Prediction. *J. Chem. Eng. Data* **2008**, *53*, 2148–2153.
- (53) Valderrama, J. O.; Forero, L. A.; Rojas, R. E. Critical Properties and Normal Boiling Temperature of Ionic Liquids. Update and a New Consistency Test. *Ind. Eng. Chem. Res.* **2012**, *51*, 7838–7844.
- (54) Jha, D.; Haider, M. B.; Kumar, R.; Balathanigaimani, M. S. Extractive desulfurization of dibenzothiophene using phosphonium-based ionic liquid: Modeling of batch extraction experimental data and simulation of continuous extraction process. *Chem. Eng. Res. Des.* **2016**, *111*, 218–222.
- (55) Dehghani, M. R. Extractive Desulfurization of Fuels Using Ionic Liquids, 2016. <https://www.iche.org/conferences/aiche-annual-meeting/2016/proceeding/paper/345e-extractive-desulfurization-fuels-using-ionic-liquids> (accessed August 22, 2020).
- (56) Lu, Y.; King, F. L.; Duckworth, D. C. Electrochemically-induced reactions of hexafluorophosphate anions with water in negative ion electrospray mass spectrometry of undiluted ionic liquids. *J. Am. Soc. Mass Spectrom.* **2006**, *17*, 939–944.
- (57) Gao, S.; Jin, J.; Abro, M.; He, M.; Chen, X. Selection of ionic liquid for extraction processes: Special case study of extractive desulfurization. *Chem. Eng. Res. Des.* **2021**, *167*, 63–72.
- (58) Gao, S.; Yu, G.; Abro, R.; Abdeltawab, A. A.; Al-Deyab, S. S.; Chen, X. Desulfurization of fuel oils: Mutual solubility of ionic liquids and fuel oil. *Fuel* **2016**, *173*, 164–171.
- (59) Azeotropic Data for Binary Mixtures, (n.d.), 2021. <https://cpbus-e1.wpmucdn.com/blogs.uoregon.edu/dist/1/8309/files/2014/10/azeotropic-data-of-binary-mixtures-1ascnny.pdf> (accessed July 12, 2021).
- (60) 8.13 Sulfur recovery, US EPA. (n.d.), 2021. https://www.epa.gov/sites/production/files/2020-09/documents/8.13_sulfur_recovery.pdf (accessed July 1, 2021).
- (61) Tian, R.; Xu, W.; Li, Y.; Tian, J.; Wu, L. Energy Consumption Analysis of a Diesel Hydrotreating Unit Using an Aspen Simulation. *Processes* **2022**, *10*, No. 2055.